

UNCLASSIFIED

AD NUMBER

AD821916

LIMITATION CHANGES

TO:

Approved for public release; distribution is unlimited.

FROM:

Distribution authorized to U.S. Gov't. agencies and their contractors;
Administrative/Operational Use; 24 OCT 1967.
Other requests shall be referred to Air Force Technical Applications Center, Washington, DC.

AUTHORITY

AFTAC USAF ltr 28 Feb 1972

THIS PAGE IS UNCLASSIFIED

AD821916

**SEISMIC DATA LABORATORY
QUARTERLY TECHNICAL
SUMMARY REPORT**

(JULY — SEPTEMBER 1967)

24 OCTOBER 1967

Prepared for

AIR FORCE TECHNICAL APPLICATIONS CENTER

Washington, D. C.

By

TELEDYNE, INC.

Under

Project VELA UNIFORM

Sponsored By

ADVANCED RESEARCH PROJECTS AGENCY

Nuclear Test Detection Office

ARPA Order No. 624

SEISMIC DATA LABORATORY
QUARTERLY TECHNICAL
SUMMARY REPORT

24 October 1967

AFTAC Project No.:	VELA T/6702
Project Title:	Seismic Data Laboratory
ARPA Order No.:	624
ARPA Program Code No.:	5810
Name of Contractor:	TELEDYNE, INC.
Contract No.:	F33657-67-C-1313
Date of Contract:	2 March 1967
Amount of Contract:	\$ 1,735,617
Contract Expiration Date:	1 March 1968
Project Manager:	William C. Dean (703) 836-7644

P. O. Box 334, Alexandria, Virginia

AVAILABILITY

This document is subject to special export controls and each transmittal to foreign governments or foreign national may be made only with prior approval of Chief, AFTAC.

The work reported herein was supported by the Advanced Research Projects Agency, Nuclear Test Detection Office, under Project VELA-UNIFORM and accomplished under the technical direction of the Air Force Technical Applications Center under Contract F33657-67-C-1313.

Neither the Advanced Research Projects Agency nor the Air Force Technical Applications Center will be responsible for information contained herein which may have been supplied by other organizations or contractors, and this document is subject to later revision as may be necessary.

TABLE OF CONTENTS

	Page No.
I. INTRODUCTION	1
II. WORK COMPLETED	
A. Matched Filtering and Array Processing Long-Period Rayleigh Waves	1
B. Beamforming the Extended E3 Subarray at LASA	3
C. Spatial Correlation of Amplitude Anomalies	7
D. Frequency and Wave Number Spectra of Vertical Arrays	11
III. SUPPORT AND SERVICE TASKS	
A. VELA-UNIFORM Data Services	15
B. Data Library	15
1. Digital Seismograms	15
2. LASA Data	15
3. Digital Programs	16
4. Analog Composite Tapes	17
C. Data Compression	17
D. Automated Bulletin Process	17
REFERENCES	18
APPENDIX A - Organizations Receiving SDL Data Services	

ILLUSTRATIONS

FIGURES

Follows Page No.

1. Map Showing Locations of LRSM & Observatory Instruments Used in This Study	1
2. Comparison of Several Signal Enhancement Procedures For A Single LASA Element (B1-LPZ)	2
3. Comparison of Several Multichannel Signal Enhancement Procedures for 21 LASA LPZ Elements	2
4. Typical results of Matched Filter Processing of LRSM (and VELA Observatory) LPZ Seismograms, & The Sum of 14 Such Matched Filter Outputs.	2
5. LASA Extended E3 Subarray	4
6. Average Noise Reduction by Beamforming Outputs of The Extended E3 Subarray	5
7. Average S/N Gain By Beamforming Six Outputs of The Extended E3 Subarray	6
8. Average Noise Reduction By Beamforming Six Outputs of The Extended E3 Subarray	6
9. Average S/N Gain By Beamforming Outputs From The Extended E3 Subarray	6
10. Average Noise Reduction In The Extended E3 Subarray For Two Experimental Methods	6
11. Average Noise Reduction In The Extended E3 Subarray For Two Experimental Methods	6
12.	9
13.	9
14. Simulated Signal Using Acoustic Log Propagation Velocities Measured at APOK	12
15. Simulated Noise	12
16. Unfiltered Noise	12
17. Unfiltered Noise	14
18. Main Pulse of The Aleutian Earthquake	14

TABLES

Follows Page No.

1. Source Data	4
2. Sensor Groups and Spacing for N=6	4
3. Sensor Groups and Spacing for N=3	5
4. Sensor Groups and Spacing for N=7	5
5. Logs of Normalized P-P Amplitudes	9
6. Subarray Correlations For The Colombia Earthquake	10
7. Correlations of Similarly Oriented Subarrays For The Colombia Earthquakes	10

I. INTRODUCTION

This quarterly technical summary report covers the work performed during the period July through September 1967. Work previously completed or currently in progress is mentioned only as it relates to analyses completed during this reporting period.

Analyses completed, for which results have been reported, are discussed in Section II under descriptive headings. Section III contains a discussion of the support and service tasks performed for in-house projects and for other VELA-UNIFORM participants. Appendix A is a listing of those organizations receiving SDL data services during this period.

II. WORK COMPLETED

A. Matched Filtering and Array Processing of Long-Period Rayleigh Waves

The matched filter technique takes advantage of the Rayleigh wave dispersion to detect the signal in the background noise. Analogous to a chirp radar the method forms a cross correlation of the previously recorded Rayleigh wave from a given epicentral region with new data recorded at that station. This cross correlation will be significant only when a second Rayleigh wave arrives with the same dispersive characteristics. The output will be a symmetrical pulse approximating the autocorrelation of the Rayleigh waveform.

Array summing is easily achieved using matched filters. Each station in a network must use its own matched filter to detect the surface waves from a given earthquake region. However, the signal output of all the stations will be pulse waveforms which are quite similar. Consequently, the array combination of these outputs over an entire network requires only the alignment of the matched filter output pulses and summing.

The data used for this experiment were two Greenland Sea earthquakes with the same epicenter; one magnitude 4.6 and one at magnitude 4.9. The surface waves from the larger event were readily detectable at LASA and the 13 LRSM stations. The map showing the locations of the 13 LRSM stations and LASA is shown in Figure 1.



Figure 1. Map Showing Locations of LRSM and Observatory Instruments Used in This Study

Figure 2 shows the Rayleigh wave from the weaker equation recorded at LASA at a single sensor and processed in various ways. The first trace is the unfiltered signal in the noise background. The second trace is the raw data filtered by a bandpass from 15 to 50 seconds period. The third trace shows the matched filter impulse responses which is the recording of the Rayleigh wave from the larger earthquake received in this particular site. The fourth trace is a matched filter output applied to the unfiltered data and the fifth trace is the same matched filter output processed through the bandpass filter. The effect of compressing all of the Rayleigh wave energy back to the same arrival time is readily noticed by the signal pulse in the matched filter output.

Figure 3 shows the similar results from the 21 long-period verticals summed together. Over an array of LASA's size the Rayleigh dispersions from a teleseismic event are similar enough so that the array can be summed before matched filtering. As a result a single matched filter can be applied to the phased sum.

Figure 4 shows the raw data and the matched filter outputs from several LRSM stations and the phased sum of 14 matched filter outputs. In all cases the matched filter output produces a single pulse which is essentially the autocorrelation of the Rayleigh wave recorded at that station. The phase sum of all such correlation produces a pulse with a significant reduction in the background noise.

From this test which used one strong Greenland Sea earthquake to detect a weak one at the same site, we concluded that:

1. By means of a matched filter, the mean signal-to-noise ratio for the surface wave on 21 LASA LPZ seismograms was increased 6 db over that of seismograms filtered with a band pass of 15 to 50 seconds period. Mean signal-to-noise improvement of 3 to 4 db was obtained for 13 LRSM stations.

2. The signal-to-noise ratio of the matched filtered seismograms was independent of whether the seismograms were pre-filtered with a band pass filter for LASA. Pre-filtering LRSM seismograms produced matched filter results about 1.5 db better than not filtering.

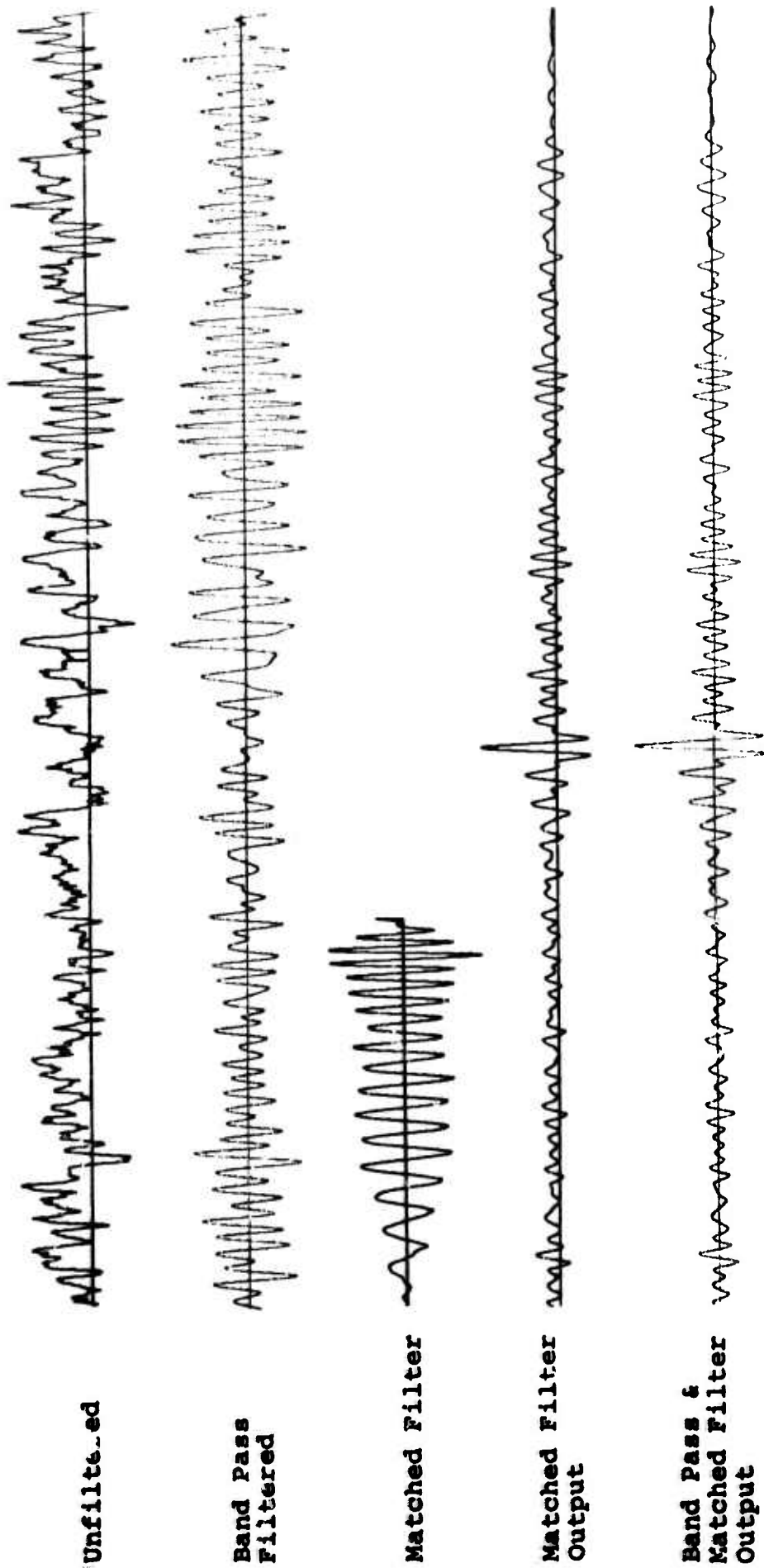


Figure 2. Comparison of Several Signal Enhancement Procedures For A Single LASA Element.
(B1 - LPZ)

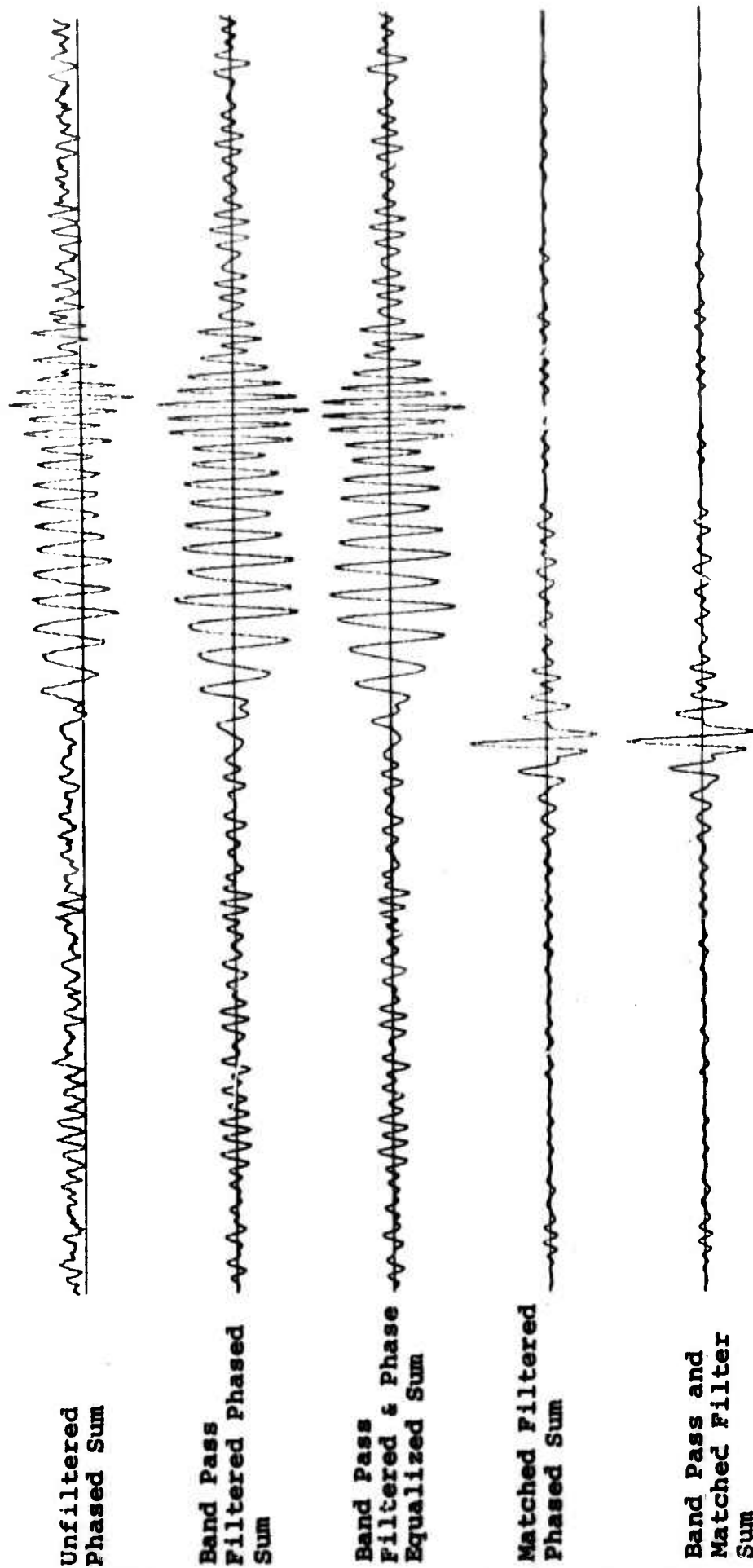
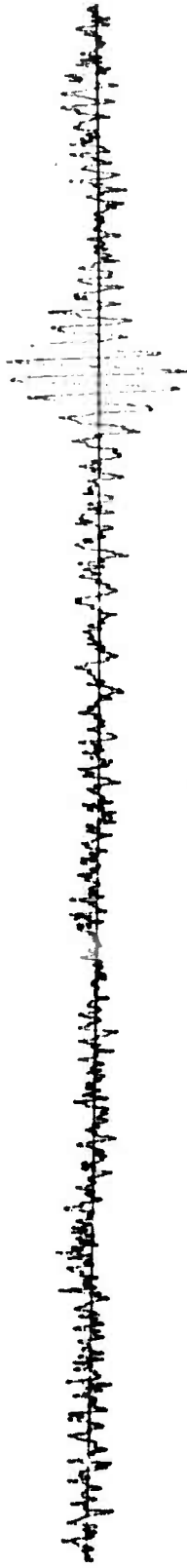


Figure 3. Comparison of Several Multichannel Signal Enhancement Procedures for 21 LASA LPZ Elements

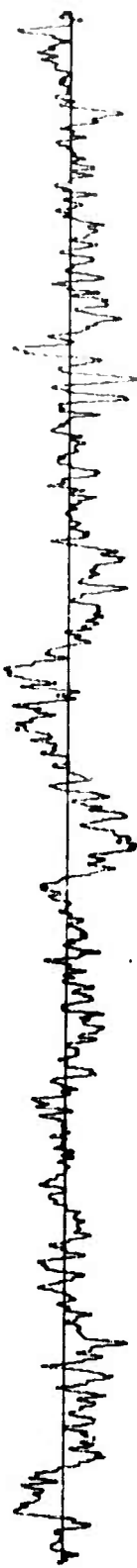
Pg-BC LPZ
Raw Data



Pg-BC Matched
Filtered



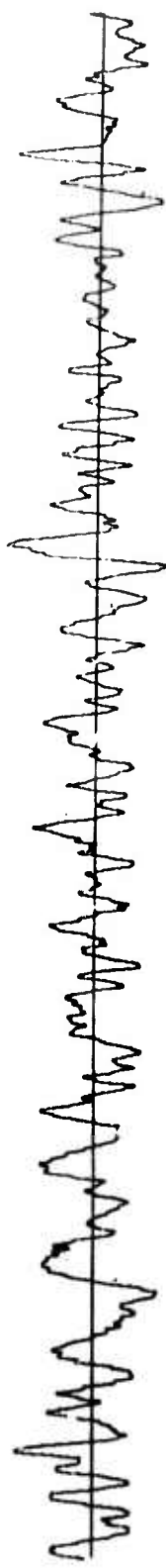
EU2AL LPZ
Raw Data



EU2AL Matched
Filtered



HN-ME LPZ
Raw Data



HN-ME Matched
Filtered



Phased Sum of
14 Matched

Filter Outputs

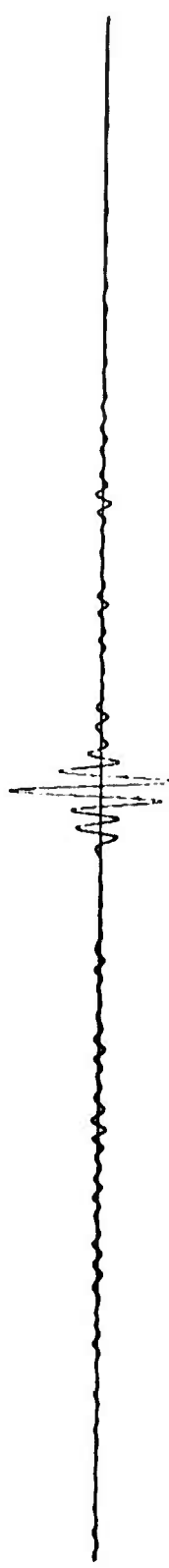


Figure 4. Typical Results of Matched Filter Processing of LRSM (& VELA Observatory) LPZ Seismograms, and The Sum of 14 Such Matched Filter Outputs

3. An additional increase of signal-to-noise approach \sqrt{N} (N = number of sensors) was achieved by phased summing the matched filter outputs for LASA if an inter-sensor spacing of at least 30 km was maintained. A similar improvement was observed for the LRSM stations which had a still larger (but not uniform) spacing.

4. For array apertures as great as the full diameter of LASA, phased equalized summations showed little increase (<1 db) in signal-to-noise over simple phased sums, both having been bandpass filtered.

5. Phased sums of matched filter outputs were consistently 7-9 db above corresponding phased sums of band pass filtered seismograms.

6. A comparison of matched filter phased sums for 13 LASA and 13 LRSM stations (spacing ≤ 30 km) showed signal-to-noise gains of 17 and 15 (16) db respectively, over the mean of individual bandpass filtered S/N values. In both cases this was within $\frac{1}{2}$ db of the value expected for uncorrelated noise.

7. Aperture at LASA causes little or no signal loss for matched filter phased sums and only moderate signal loss (.5 to 3 db) on bandpass filter phased sums for apertures up to 200 km. There was also little or no signal loss on phase summing the LRSM matched filter seismograms over a continental size aperture.

8. Even for the sensor spacings at which signal-to-noise gains were below those expected for uncorrelated noise, the percentage increase in signal-to-noise adding additional sensors was approximately the same as for the uncorrelated case.

B. Beamforming the Extended E3 Subarray at LASA

Short-period seismograms representing nine tele-seismic earthquakes recorded by vertical component instruments in the extended E3 subarray at the Montana LASA were bandpass-filtered and beamformed to determine the effect on average input signal-to-noise ratio, signal, and noise.

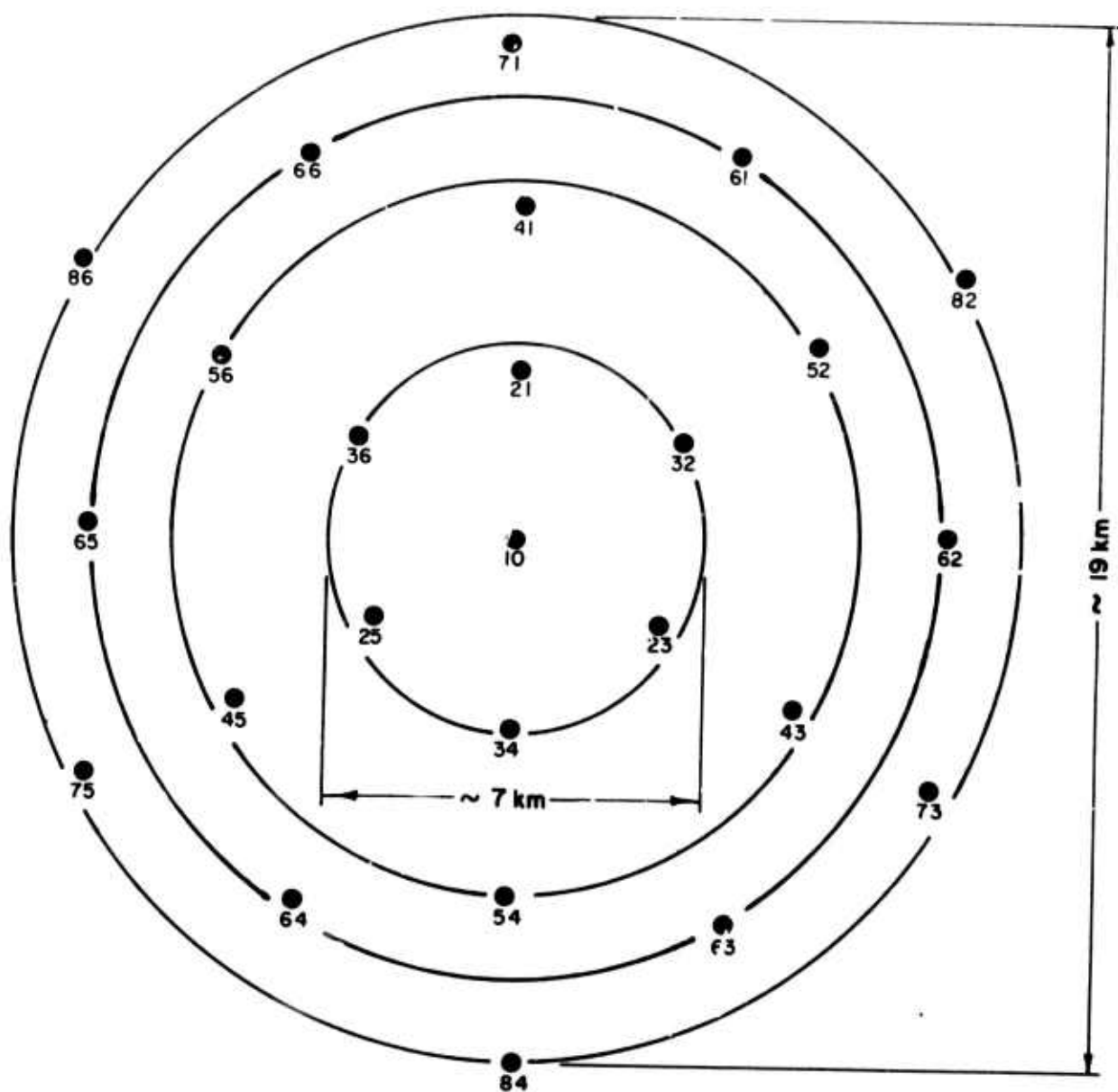
The data used in this study are nighttime recordings, occurring over a two month period, January-March, 1967. We refer to the enlarged E3 subarray which has been in operation since December 1966. This subarray has a diameter of 19 kilometers, and contains 25 sensors with spacings 3 kilometers, as shown in Figure 5. The source data shown in Table 1 were taken from P.D.E. cards furnished by the USC&GS. All outputs were bandlimited either in the range 0.4-3.0 cps or 0.6-2.0 cps, using 4-Pole Butterworth recursive filters.

Beamforming

Two procedures were used in selecting data to be beamformed. Our objective in the first was to evaluate the performance of the extended array, and we concerned ourselves with varying the number of inputs, N , to a beam as opposed to evaluating the effect of inter-sensor spacing, Δ . Beams were formed on P arrivals using data prefiltered to the band 0.4-3.0 cps for N equal to 6, 12, 13, 18, 19, and 25. These correspond to traces recorded in the outer (or inner) ring, outer 2 rings, inner two rings plus the center, outer 3 rings, inner three rings plus the center, and the entire subarray. We have already pointed out that a uniform distribution of sensors was not considered in beamsteering these data. Consequently, it follows that about the only meaningful reference to spacing is relative to the minimum separation of sensors contributing to the beams discussed above are 9.5 or 3 (outer ring or inner ring, respectively), 4.7, 3, 3, 3, and 3.

A similar procedure was used for each of nine events to determine the average effect of a variable number of beam inputs (N) on signal loss, rms noise reduction, noise power reduction at 1 cps, and signal-to-noise ratio enhancement, each quantity being referred to a mean taken from the input traces.

Table 2 (lists four sets of traces contributing to beams containing six inputs each ($N=6$), where each set represents traces recorded on an individual ring of the subarray. This procedure was our first attempt at holding N constant and varying Δ , in this instance a circumferential measurement.



INNER CIRCLE REPRESENTS SIZE OF ORIGINAL E3

Figure 5. LASA Extended E3 Subarray

Table 1. Source Data

Event Name	Date	Origin Time	Location		Distance	
			Lat.	Long.	DEG	KM
HONSHU	02 Mar 67	08:17:44.5	35.7 N	139.9 E	79.1	2793
KURILE	05 Mar 67	09:55:15.0	46.8 N	152.7 E	64.4	7165
NORTH PACIFIC	08 Mar 67	05:13:34.0	24.4 N	142.8 E	86.0	9564
HONSHU	10 Mar 67	01:54:17.5	32.4 N	137.7 E	82.8	9204
NORTH ATLANTIC	11 Mar 67	03:05:24.0	55.9 N	34.5 W	44.3	4923
HOKKAIDO	17 Mar 67	02:22:37.9	42.0 N	142.5 E	73.0	8119
FOX	17 Mar 67	06:47:40.9	53.6 N	165.3 W	37.5	4170
JUJUY	17 Mar 67	11:17:19.0	21.2 S	67.7 W	75.6	8408
SHIKOKU	19 Mar 67	02:54:22.4	28.0 N	130.5 E	90.0	10012

P-pth in KM	Apparent Velocity	Back Azimuth	Cal Date	USC & GS Mag
75	20.3	310.7	11 Jan 67	4.6
33	16.9	311.5	11 Jan 67	4.4
33	22.3	301.4	11 Jan 67	4.5
377	21.2	309.9	11 Jan 67	4.4
33	13.9	50.1	11 Jan 67	4.7
57	19.0	313.4	11 Jan 67	4.7
44	13.1	303.0	11 Jan 67	4.4
189	19.6	143.0	11 Jan 67	4.2
48	23.2	312.3	11 Jan 67	4.9

Table 2. Sensor Groups and Spacing for N=6

~Circumferential Spacing (km)				
Contributing Sensors	3*	6*	8*	9*
	21	41	61	71
	32	52	62	82
	23	43	63	73
	34	54	64	84
	25	45	65	75
	36	56	66	86

* Plots Are Averages Taken Over Seven Events

Seven of the original nine events were used to obtain average values. The procedures discussed thus far were extended to include power spectra based on individual channels and sum traces. Spectral estimates were computed over 60 seconds of noise (1200 digital points) using 120 lags.

In the second part of the study we used seismograms recorded during the night of 17 March 1967 to establish a relationship between inter-sensor spacing and noise reduction. Two experimental methods were used to determine noise reduction by beaming either three or seven traces; the first method relied on the zero lag autocorrelations and cross-correlations as described in the following section, while the second consisted of trace summation. In the case of $N=3$, uniform sensor spacings of 3, 4, 6, 8, 9, 10, 14, and 16 kilometers were used and for $N=7$ separations of 3, 6, 8, and 9 kilometers were employed. Solutions were obtained for data limited to the band 0.4-3.0 cps after which we repeated the process with traces prefiltered to 0.6-2.0 cps.

In Tables 3 and 4 we have listed sensors which contributed to 3-element and 7-element beams respectively. As shown in Table 3 outputs from either 2 or 6 beams were used to compute average noise reduction values. Referring to Table 4, we note that only one beam for each spacing was used to describe noise behavior.

The results describe the effectiveness of beam-steering outputs from the extended E3 subarray (Figures 6, 7, 8, and 9), and the effect of inter-sensor spacing on short-period beamforming results (Figures 10 and 11).

Figure 6 is a plot of noise reduction, either rms or power at 1 cps, as a function of N . The figure illustrates four significant points: first, N^2 reduction is obtained for noise power at 1 cps only in the case of $N=6$ (the outer ring); second, the reduction of rms noise levels never quite reached N^2 ; third, noise reduction is less favorable, relative to N^2 , for greater N ; and fourth, beams made of outputs from the outer ring(s) yield more noise reduction than those consisting of traces recorded in the inner ring(s). The last result is explained by the fact that inter-sensor spacing tends to be greater on the outside rings, and the noise is therefore less correlated between adjacent sensors.

Table 3. Sensor Groups and Spacing for N=3

Spacing (km)									
3*	4*	6*	8*	9*	10**	14**	16**	Contributing Sensors	
10	54	10	10	10	52	62	71		
21	63	41	63	71	54	64	73		
36	64	56	64	86	56	66	75		
10	43	10	10	10	41	61	82		
21	62	41	62	71	43	63	84		
32	63	52	63	82	45	65	86		
10	52	10	10	10					
23	61	43	61	73					
32	62	52	62	82					
10	41	10	10	10					
23	61	43	61	73					
34	66	54	66	84					
10	56	10	10	10					
25	65	45	65	75					
34	66	54	66	84					
10	45	10	10	10					
25	64	45	64	75					
36	65	56	65	86					

*Plots Are Averages Taken Over six Beams

** Plots Are Averages Taken Over Two Beams

Table 4. Sensor Groups and Spacing for N=7

Spacing (km)				
Contributing Sensors	3	6	8	9
	10	10	10	10
	21	41	61	71
	32	52	62	82
	23	43	63	73
	34	54	64	84
	25	45	65	75
	36	56	66	86

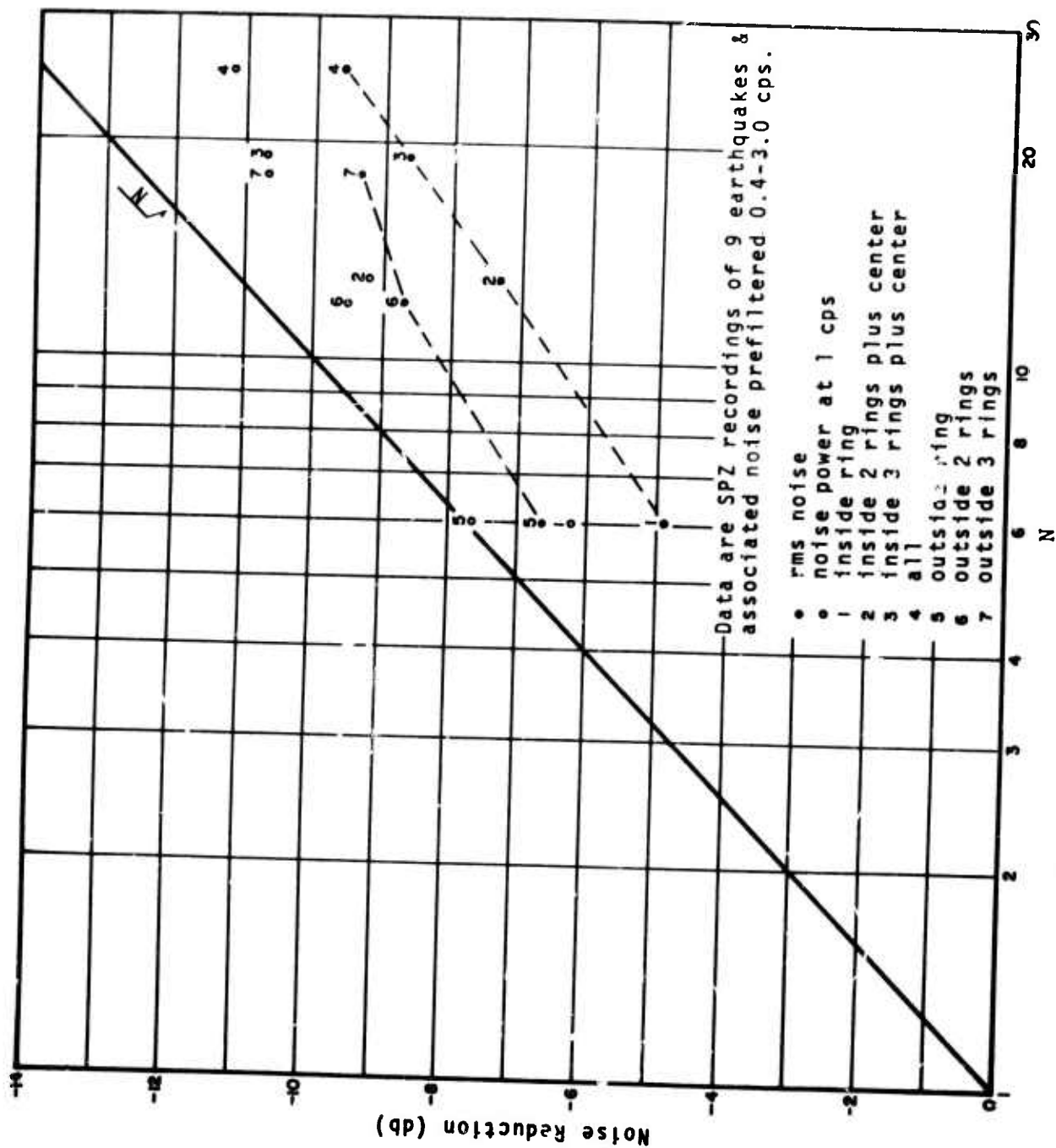


Figure 6. Average Noise Reduction by Beamforming Outputs of The Extended E3 Subarray

Figure 7 shows average signal-to-noise gain as a function of N . Here we see immediately that N^2 enhancement is never achieved, due largely to the fact the rms noise reduction falls short of N^2 as shown by Figure 6, and partly because 1-2 db of signal is lost in the beamforming process. We further note that enhancement is less favorable relative to N^2 for larger N , and that the outer ring(s) yield better results than the inner ring(s).

Figures 8 and 9 show noise reduction and signal-to-noise enhancement versus sensor spacing for $N=6$. In this case beams were formed using outputs from individual rings so that values plotted at $\Delta = 3$ km correspond to data recorded on the inside ring, $\Delta = 6$ the second ring, $\Delta = 8$ the third ring, and $\Delta = 9.5$ km the outside ring; these spacings could more appropriately be called "minimum" intervals. As shown in Figure 8, noise power at 1 cps is reduced by N^2 in the Δ interval 6-8 kilometers, and rms noise is reduced to within 1 db of N^2 at $\Delta = 6$ and remains reasonably constant thereafter. On the other hand, signal-to-noise enhancement (Figure 9) reaches a maximum, + 5 db, at $\Delta = 6$ and remains essentially constant beyond. Once again we are reminded that imprecision in the beamforming process accounts for 1-2 db signal loss.

We turn now to examples of beamforming in which N has been held constant and spacing between adjacent sensors has been changed from a minimum of 3 km to a maximum of 16 km (Figures 10 and 11). Data plotted on Figure 10 were prefiltered to 0.4-3.0 cps, while those shown in Figure 11 were bandlimited in the range 0.6-2.0 cps. In both figures the dashed curves represent results for noise reduction based in part on the average of the noise mean squares whereas the plotted points are based on the average rms value input to the beam. Referring to Figure 10, we note that the minimum sensor spacing indicated by either experimental method for $N=3$ or $N=7$ is about 6 km, if N^2 noise reduction is desired. Actually, values based on average rms reach N^2 reduction at 8 or 9 km. It is important to remember that the plotted data for $N=3$ are really averages of either two or six beams, whereas, each plot for $N=7$ was taken from a single beam. As shown in Figure 11, the minimum spacing indicated for data prefiltered 0.6-2 cps is about 5 km, and rms values reach N^2 at about 8 km spacing.

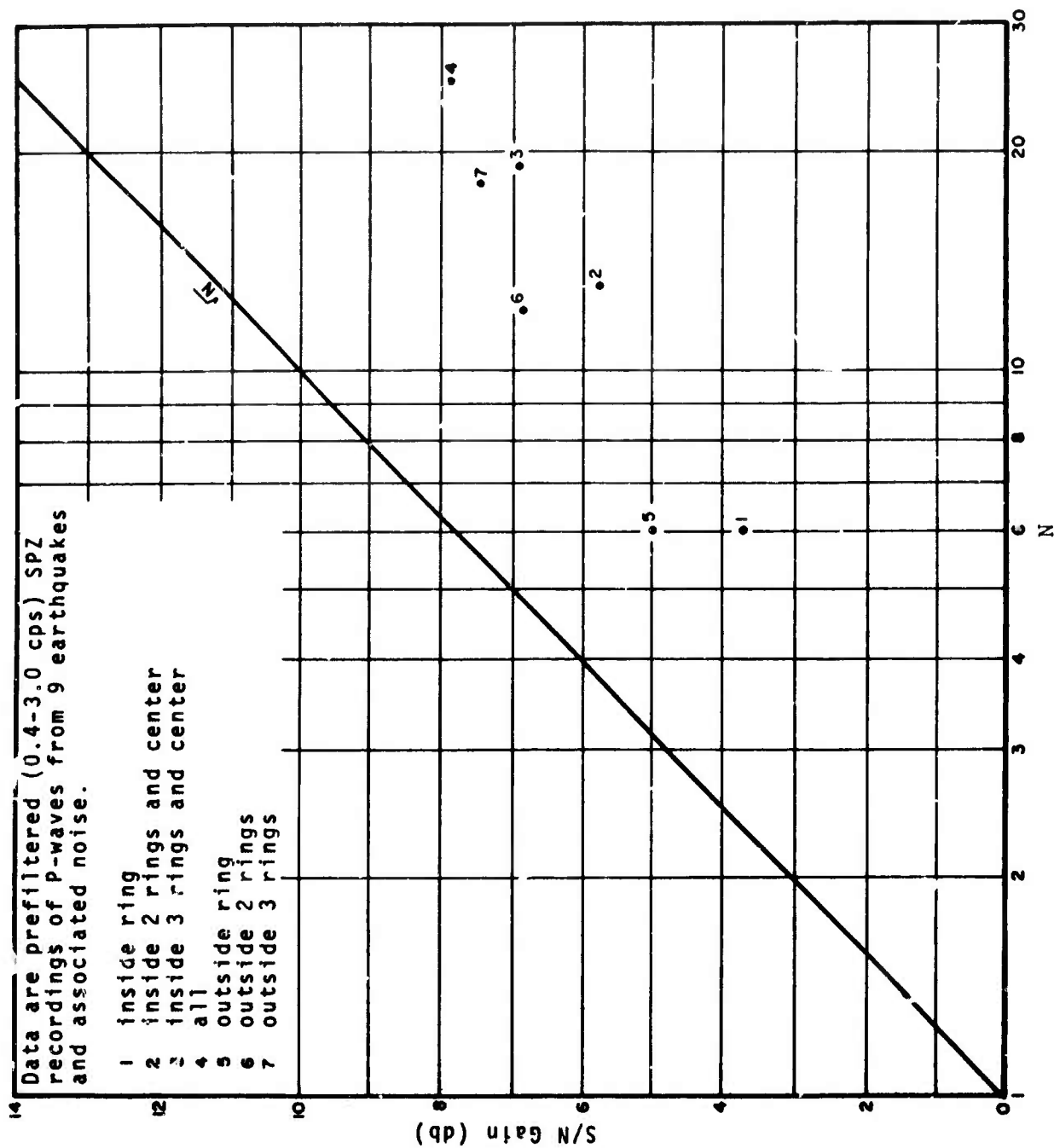


Figure 7. Average S/N Gain By Beamforming Six Outputs of The Extended E3 Subarray

Data are SPZ recordings of 7 earthquakes & associated noise prefiltered 0.4-3.0 cps.

N=6

- rms noise
- noise power at 1 cps
- 1 inside ring
- 2 second ring
- 3 third ring
- 4 outside ring

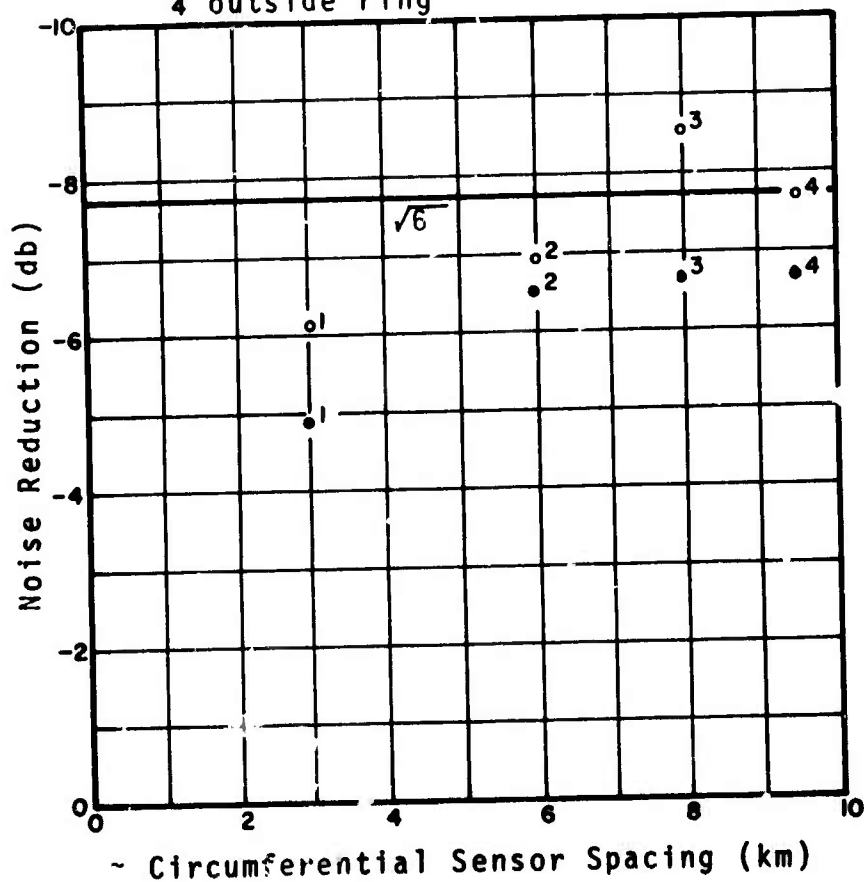


Figure 8. Average Noise Reduction By Beamforming Six Outputs of The Extended E3 Subarray

Data are SPZ recordings of 7 earthquakes &
associated noise prefiltered 0.4-3.0 cps.
N= number of outputs summed = 6

- 1 inside ring
- 2 second ring
- 3 third ring
- 4 outside ring

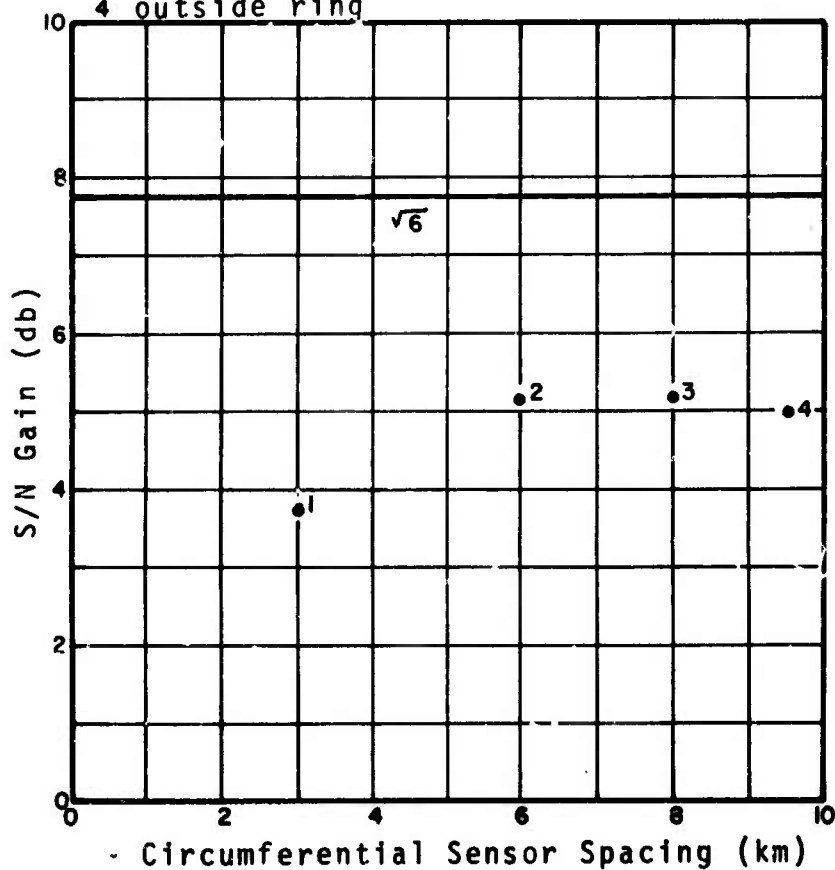


Figure 9 . Average S/N Gain By Beamforming Outputs
From The Extended E3 Subarray

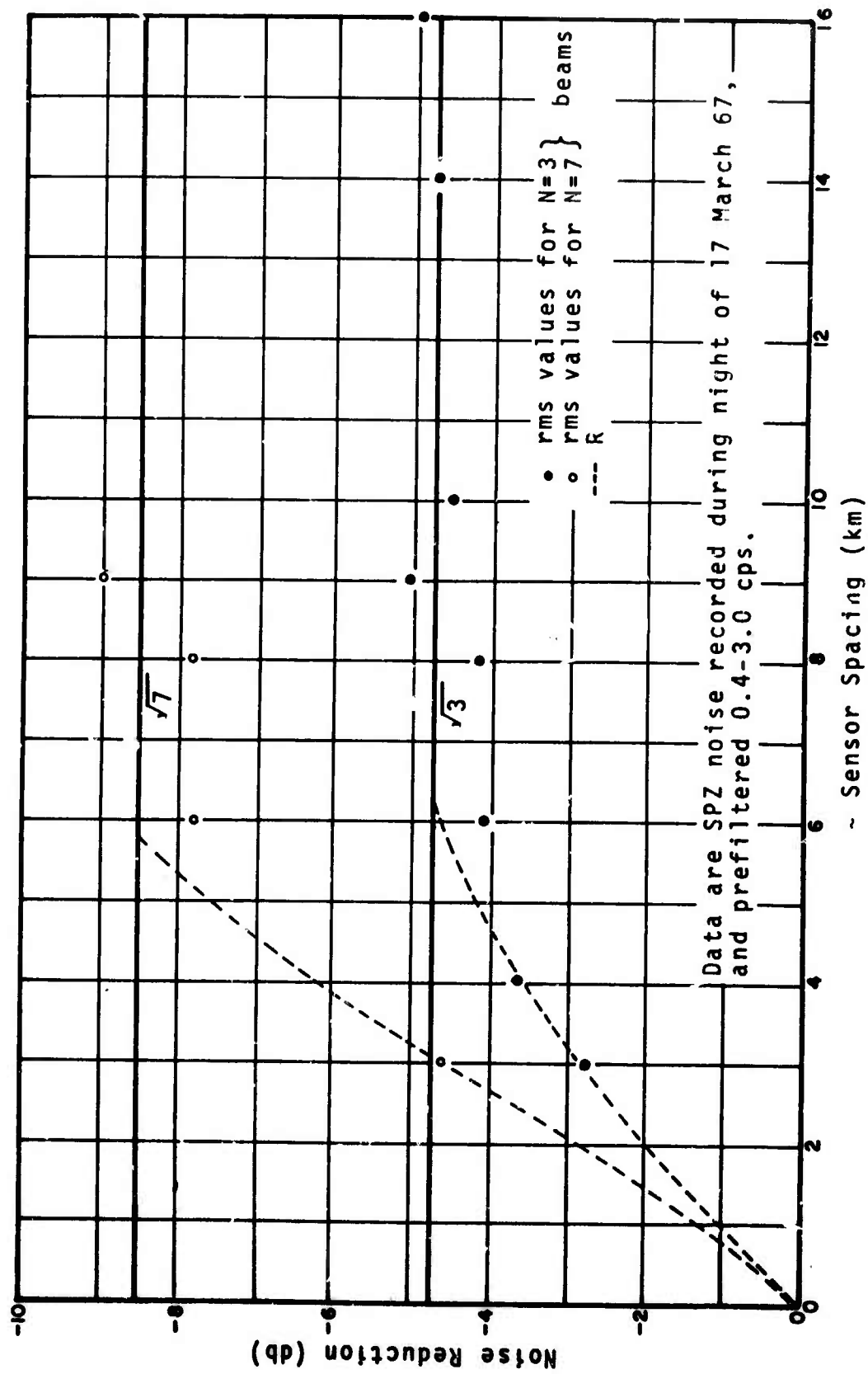


Figure 10. Average Noise Reduction In The Extended E3 Subarray For Two Experimental Methods.

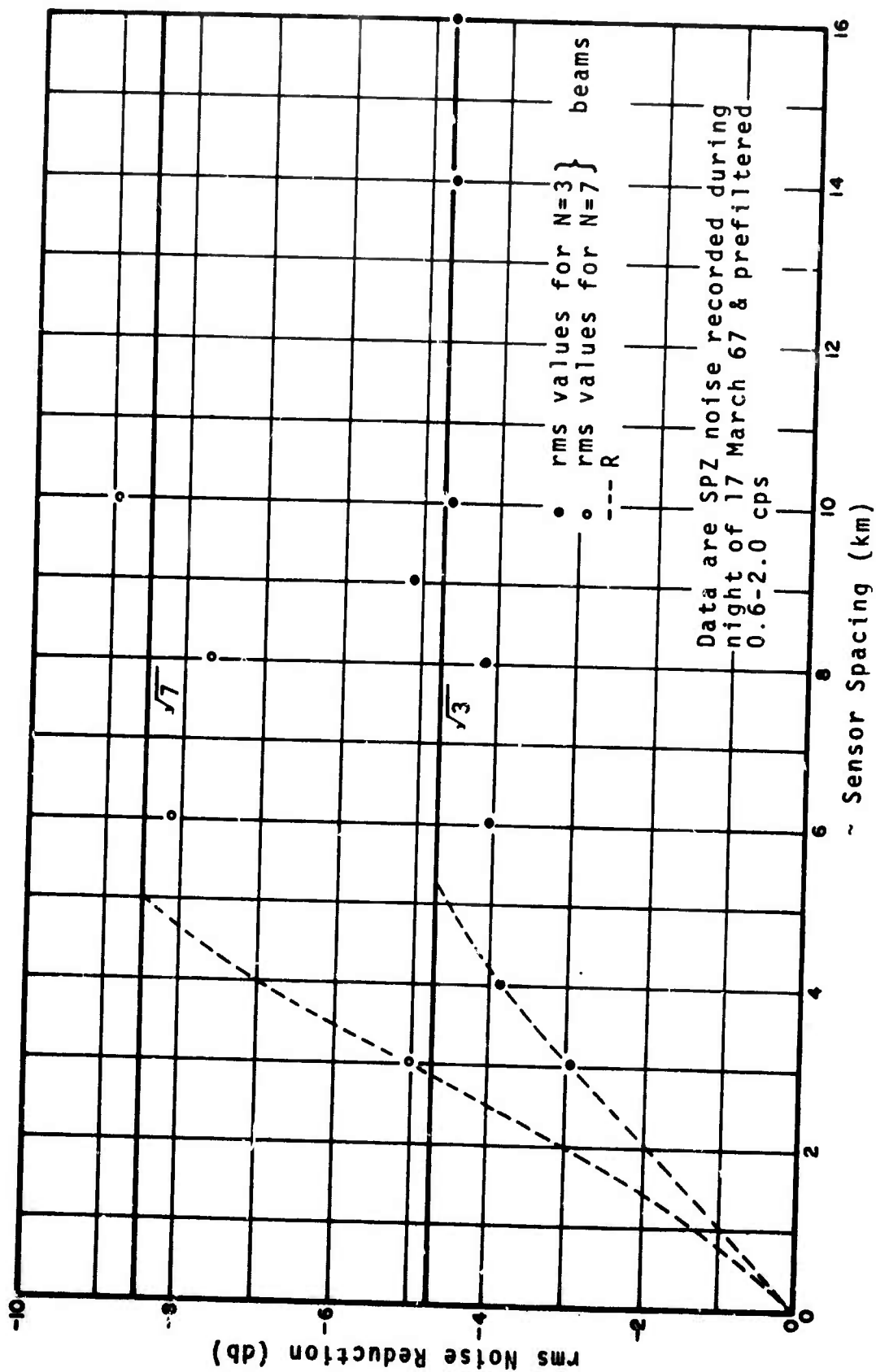


Figure 11. Average Noise Reduction In the Extended E3 Subarray For Two Experimental Methods

The following conclusions are based on the results of a beamforming study which used short-period vertical-component seismograms recorded during January-March 1967 in the extended E3 subarray at the Montana LASA. With the exception of beams made up of seven inputs, our results represent averages taken from several beams.

Beams consisting of prefiltered (0.4-3.0 cps) inputs from the entire extended E3 subarray do not yield $N^{\frac{1}{2}}$ improvement in signal-to-noise ratio. This is due primarily to the fact that noise is partly correlated between adjacent sensors and therefore is not reduced by as much as $N^{\frac{1}{2}}$, and partly to signal losses accompanying the beamforming process.

If input data are prefiltered to 0.4-3.0 cps, beams composed of six traces reduce noise by approximately $N^{\frac{1}{2}}$ when element spacings are equal to or greater than 6 kilometers.

For data prefiltered 0.4-3.0 cps, beams consisting of either 3 or 7 inputs reduce the average of the noise mean squares and average rms noise approximately by $N^{\frac{1}{2}}$ at a minimum sensor separation equal to or greater than 6 kilometers. If the data are prefiltered 0.6-2.0 cps, the minimum spacing is reduced to about 5 kilometers.

Average signal loss due to imprecise beams amounts to 1-2 db.

C. Spatial Correlation of Amplitude Anomalies

Spatial correlations of amplitude anomalies have been conducted over LASA and LASA subarrays to test the hypothesis that these anomalies exhibit spatial stationarity.

It has been demonstrated^(1,2) that the normalized short period peak-to-peak amplitudes of teleseismic events have a log normal distribution. That is, if the amplitudes of a set of events from the same geographic region are measured and their logarithms are taken, then we find that

$$\log a_{ij} = \log L_{ij} - \frac{1}{N} \sum_{j=1}^N \log L_{ij},$$

has a normal distribution. In this equation, the L_{ij} are either the measured peak-to-peak amplitudes at all elements in a LASA subarray or are the peak-to-peak amplitudes observed at the center elements of the subarrays. The index j is on the seismometer and i is an event index.

The distribution of log amplitudes is not normal if the collection includes all elements in LASA. The variance of $\log a_{ij}$ is larger in the case where the L_{ij} are the observed amplitudes at the center elements. The variances are the same at each subarray when the L_{ij} are the amplitudes of the elements in a subarray. Thus, these variances can be pooled after normalization.

The anomalies are assumed to be real in that a precisely repeated event should produce the same amplitudes at the seismometers as the original. The anomalies vary however for events from the same geographic region and it is unlikely that a calibration of the earth would be a practical procedure with which to eliminate anomaly effects. Rather, a statistical approach seems to be more reasonable.

The fact that the anomalies in the subarrays can be pooled after normalization suggests that one may successfully hypothesize that these anomalies exhibit spatial stationarity. That is, although there may be slowly varying effects with distance, with these removed the expectation of a particular amplitude anomaly is independent of spatial location.

Further we wish to test whether the anomaly process is covariance stationary. If so, then the covariance function will serve as a measure of the distance which should be placed between seismometers so that they will exhibit independent amplitude estimates. Moreover, since the anomalies are log-normal, so another statistic is needed. The covariance function is a complete statistic for normally distributed variables.

To test the possibility of correlation among the peak-to-peak amplitudes across all of LASA we selected signals from eleven Fiji Island earthquakes which occurred at 243° azimuth and from 9,500 km to 10,500 km distance from the center of LASA. From these eleven events, correlation coefficients were computed as spatial displacements were made over LASA. In the computations, the logarithms of the event amplitudes have been normalized so that anomalies from all subarrays have a common mean. We define the estimate of the coefficient of correlation to be

$$r = (\sum X_i Y_i) / (\sum X_i^2)^{1/2} (\sum Y_i^2)^{1/2}.$$

Since all eleven events were relatively closely grouped in comparison to the overall path, the average of the logarithms of the normalized peak-to-peak amplitudes at a given subarray was used as an estimate of the true value for that subarray (Table 5).

These average values were used in the calculations of the spatial correlation coefficients. Correlations were computed along a line parallel to the incoming signal (243° az.) and another set along a line perpendicular to the incoming signal (153° az.). Due to the configuration of LASA, few displacements exist where enough subarrays intersect to compute a valid coefficient of correlation. Figure 12 presents the coefficients of correlation plotted against the spatial shifts using the average logarithm of the normalized peak-to-peak amplitudes over all events as the estimate of the true value for each subarray.

The correlation coefficients for the individual events were computed. That is, each event was considered singly as the spatial shifts were made across LASA at 153° and 243° azimuth. Figure 13 presents the graph of \bar{r} vs. the spatial shifts. It is of interest to compare the graphs of Figures 12 and 13, i.e the coefficient of correlation of the average coefficient of correlation of the individual events vs. displacement.

Table 5. Logs of Normalized P-P Amplitudes

Subarray Designation	Event Number	152	171	197	219	238	247	253	254	271	342	359	AVG.LOG.
B1	-.086	.143	-.022	-.108	.140	.057	.061	-.168	.033	-	-	.086	.014
B2	.065	.013	.061	-.260	-.018	-.009	-.056	.013	-.125	-	-	-.125	-.044
B3	.061	.061	-.097	.137	.068	.137	.045	.041	-.041	-	-	.017	.043
B4	.100	.230	.310	-.027	.025	.104	.299	.041	.117	-	-	.204	.140
C1	-.013	-.013	-.097	-.036	.283	.146	.086	.134	.274	-.092	-	-	.067
C2	-.292	-.102	-	-	-.495	-.310	-.208	-.208	-.276	-	-	-.125	-.224
C3	-.066	.161	-.097	.107	.107	.057	-.155	.065	-.041	-	-	.228	.037
C4	.009	-.137	-.398	-.027	.258	.093	.104	.076	.068	-	-	-.027	.002
D1	.193	-.013	.310	.369	.408	.270	-.027	.204	-	-	.100	-	.202
D2	-.244	-	-.301	-	-.125	.045	-.081	-	-	-	-	-	-.141
D3	.041	-.041	.253	.009	-.276	-	-	-	-	-	.283	.086	.051
D4	-.229	-.377	-	-.284	-.018	-.187	-.086	-.013	-.032	-.168	-.168	-.071	-.147
E1	-	-.137	-	-.041	-.125	-.187	-.284	-	-.125	-.032	-.032	-.252	-.148
E2	-	-.071	-	-	-.495	-.252	-	-.585	-.161	-.066	-.066	-.125	-.251
E3	.009	-.444	-	-.108	-.367	-	-.051	-.018	-	-.420	-	-	-.200
E4	.076	.427	-.046	.124	.350	-.009	.155	.170	.230	.004	.004	-	.148
F1	-	-	-	-	.107	-.108	-	-	-.149	-	-	-.181	-.083
F2	.223	.230	-.071	-.102	.107	-.009	-.004	-.027	-.086	.188	.188	.086	-.049
F3	.352	.179	.277	.161	.204	.223	.250	.188	.086	-	-	.297	.222
F4	-.143	-.215	-.022	-.009	-	-.125	-.161	-.081	.152	.025	.025	-.125	-.070
AO	-.066	.104	-.046	.093	-.125	.057	.107	.167	.076	.179	.179	.017	.051

Logs of Normalized P-P Amplitudes

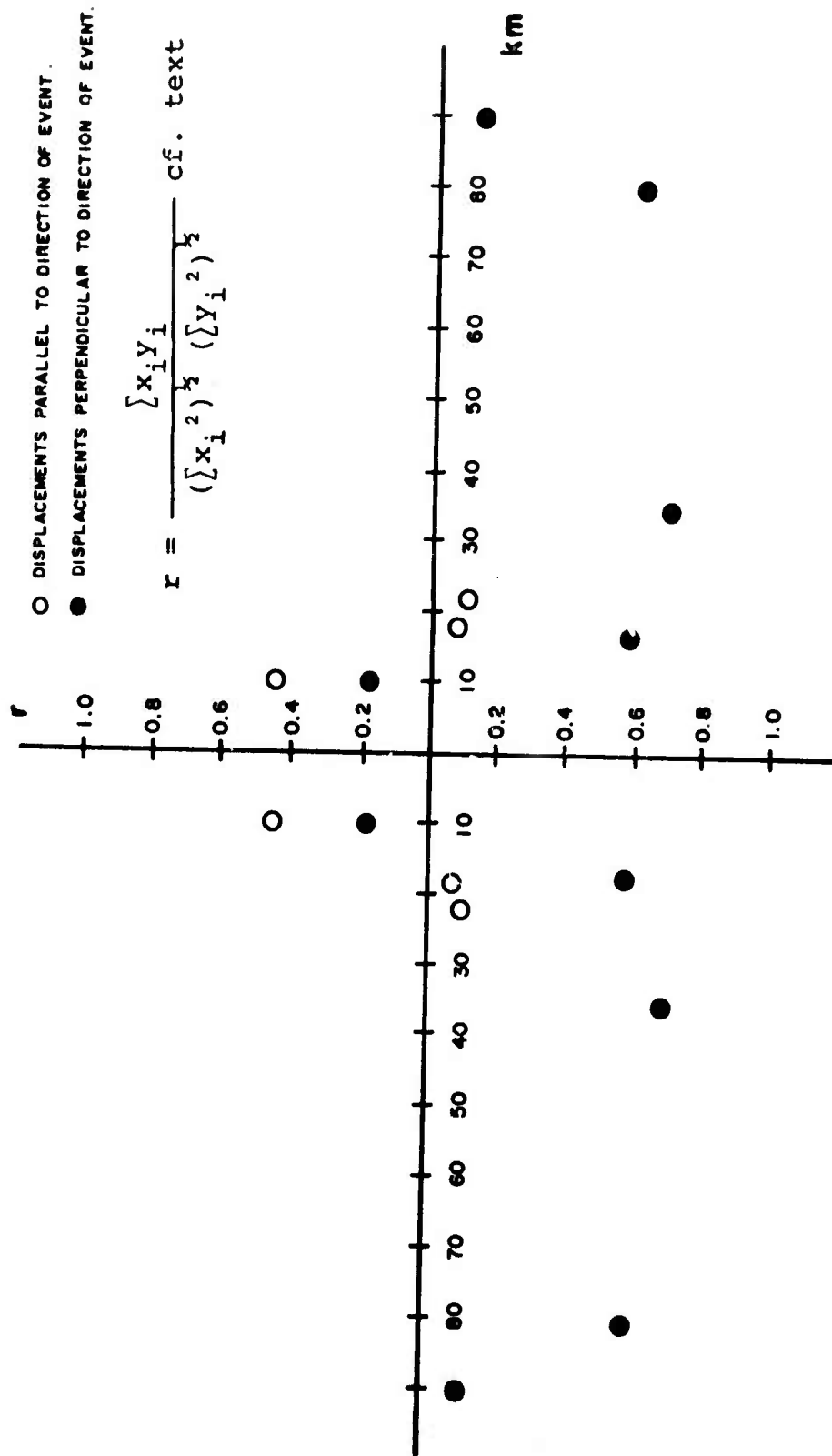


Figure 12.

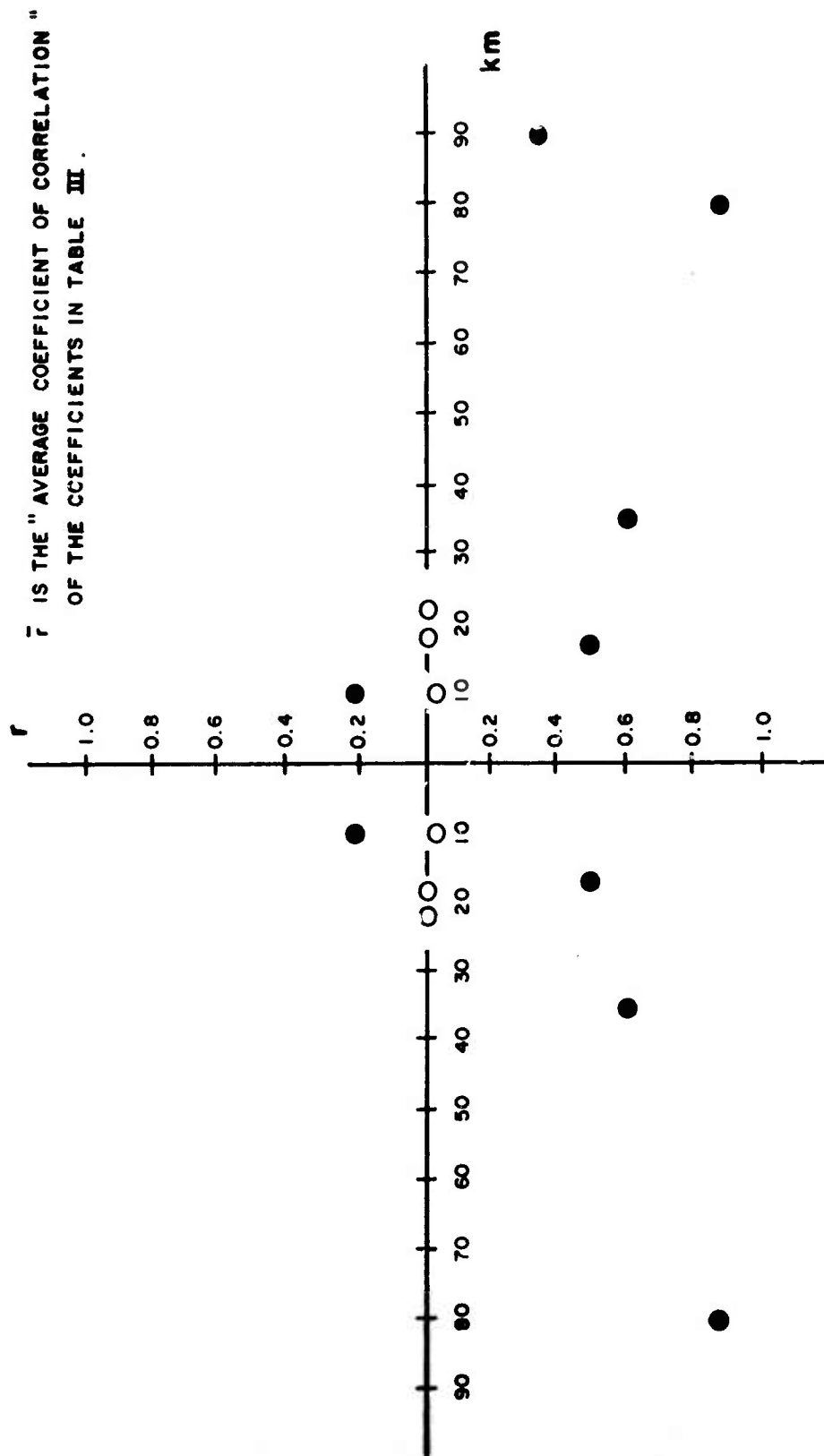


Figure 13.

After examining correlations over all LASA, we directed our attention to spatial correlations over subarrays. The concept of spatial shifting over a subarray is the same as that over all of LASA except that unlike LASA the configuration of a subarray is well defined in terms of concentric circles and radial spokes every 60° . The spatial shifts over the subarrays were made along the legs (radial spokes) in this instance rather than with respect to the origin of the event.

Three N. Colombia events (21 Dec. 65; 21 April 66; 12 June 66) were chosen on the basis of availability of complete tapes of all 525 instruments in LASA for events which originated very close together. Again the logarithms of the normalized data were used to compute the coefficient of correlation, and the means of the data samples were set to zero. As spatial displacements were made across each subarray (at 0.5 km increments), coefficients of correlation were computed and graphs of coefficients vs. displacement were drawn for each leg for every subarray. The patterns in the graphs were cross-checked among the same subarrays for all three events and among similarly oriented subarrays for the same event. No consistent relationships were discovered with this approach. Contouring seemed to suggest certain patterns (viz., that the contour "pointed" towards the direction of the event) and some consistencies were found, but the presence of exceptional and contradictory contours made such a conclusion at best doubtful.

Coefficients of correlation were computed over each subarray for paired events using the normalization described earlier the equation. That is, the twenty-five readings of the A subarray for, say, the 21 December 1965 earthquake, were tested against the respective twenty-five readings of this subarray for, say, the 21 April 1966 earthquake. The three independent earthquakes yield three distinct pairs for testing in this manner, and each pair of events has a maximum of twenty-one coefficients to be computed--one coefficient corresponding to each subarray.

In nearly every case, the coefficient was significant (i.e. correlation existed) and in many cases (nearly two-thirds) the coefficients were between .8 and 1.0. Table 6 summarizes the results of these calculations. This test can be

Table 6. Subarray Correlations For The Colombia Earthquakes

	21 Dec 65 21 Apr 66		21 Dec 65 12 Jun 66		21 Apr 66 12 Jun 66	
	Computed r	Critical r, 5%	Computed r	Critical r, 5%	Computed r	Critical r, 5%
B1	0.693	0.388	0.613	0.388	0.537	0.388
F3	0.955	0.388	0.851	0.388	0.776	0.388
F4	0.987	0.388	-0.477	0.388	-0.503	0.388
A0	0.418	0.388	0.637	0.388	0.235	0.388
E3	0.815	0.388	0.754	0.388	0.959	0.388
C4	0.733	0.396	0.933	0.388	0.943	0.396
B4	0.815	0.388	0.754	0.396	0.790	0.396
C1	0.939	0.388	0.893	0.388	0.844	0.388
C2	0.898	0.388	0.782	0.388	0.639	0.388
B2	0.857	0.388	0.767	0.388	0.945	0.388
C3	0.902	0.388	0.746	0.388	0.836	0.388
D3	0.986	0.388	0.977	0.388	0.979	0.388
D4	0.563	0.388	0.368	0.388	0.634	0.388
D1	0.831	0.404	0.882	0.404	0.931	0.388
D2	0.412	0.396	0.452	0.388	0.511	0.396
E3	0.945	0.388	0.815	0.388	0.843	0.388
E4	0.450	0.388	0.511	0.388	0.805	0.388
E1	0.900	0.388	0.825	0.388	0.806	0.388
F1	0.956	0.388	0.916	0.388	0.898	0.388
E2	0.873	0.388	0.889	0.388	0.901	0.388
F2	0.956	0.388	0.860	0.388	0.860	0.388

Subarray correlations for the Colombia earthquakes

The critical values are determined by using the "t" distribution where

$$t = r \left(\frac{n-1}{1-r^2} \right)^{1/2}$$

A detailed explanation is presented in Snedecor's "Statistical Methods" Fifth Edition, pp 173, 174.

Table 7. Correlations of Similarly Oriented Subarrays
For The Colombia Earthquakes

	<u>21 Dec. 1965</u>		<u>21 Apr. 1965</u>		<u>12 Jun. 1965</u>	
	Computed r	Critical $r, 5\%$	Computed	Critical $r, 5\%$	Computed r	Critical $r, 5\%$
C4, E1	0.239	0.388	0.232	0.396	0.121	0.388
B1, C2	0.082	0.388	0.060	0.388	0.257	0.388
B1, D2	0.200	0.388	-0.068	0.396	0.239	0.388
B1, E3	0.332	0.388	0.195	0.388	0.495	0.388
C2, D2	-0.137	0.388	-0.137	0.396	-0.340	0.388
C2, E3	0.005	0.388	-0.033	0.388	0.143	0.388
D2, E3	0.227	0.388	0.042	0.396	0.108	0.388

considered as examining the correlation among the instrument responses as the source distance is varied. In the next step, the converse of this procedure was done -- the respective elements for similarly oriented subarrays (account being taken for long and short configurations) were inspected for correlation for each earthquake. This time, correlations were not detected with the exception of one case which may be ascribed to chance (Table 7).

Only tentative conclusions can be drawn from this data. The sparse sampling of the LASA array limits the reliability of the correlation coefficients which were computed. For this reason a uniformly spaced grid of seismometers would have aided this study.

It is likely that the anomaly process cannot be considered to be spatial covariance stationary. Since this process is, in fact, a description of the underlying geology, one might have hypothesized this from the beginning. We do not have a simple explanation for the log-normal distribution of the anomalies or for their apparent stationarity other than this effect also reflects the geology.

D. Frequency and Wave Number Spectra of Vertical Arrays

We have written a new program to compute the f-k spectra for vertical arrays (VFKSPTRM). The normal f-k spectra for surface arrays must consider two space variables and one time variable. The Fourier transform of the three-variable function (signal spectra, noise spectra, and array response) leads to two wave number variables, k_x , k_y and one frequency variable. To plot three-dimensional f-k spectra on a two-dimensional page our normal practice is to plot a contour map of the f-k spectra as a function of k_x and k_y at one particular frequency.

The vertical array has one less dimension than a surface array. Consequently, a contour map of vertical array responses can exhibit all the pertinent variables simultaneously. The new SDL program plots frequency on the vertical axis and wave number on the horizontal axis. As in the case of the surface arrays, the impulse response of a vertical array assumes an input with a constant frequency spectra. The normal contour plot of the f-k spectrum for an impulse will show no variation in the frequency variable. Thus the entire impulse response of the array can be indicated by a strip at the bottom of each f-k spectra computed.

To demonstrate the f-k spectrum program, we show on Figure 14 the f-k spectrum of a synthetically generated signal. The signal model is generated with 1.25 cps pulse using an 0.8 second echo at the source and with a receiver echo delayed by using appropriate uphole times obtained from the propagation velocity observed at APOK. The reflection coefficient at the surface is assumed to be 0.9. The split peak in the spectrum is due to the source echo which nulls at 1.25 cps.

An example of an f-k spectrum for some synthetically generated noise at APOK is shown on Figure 15. Noise is simulated by taking random numbers from a Gaussian population and passing them through a filter tuned to 0.25 cps and 2.0 cps to obtain noise similar in spectral characteristic to that observed at APOK. The model of the noise at underlying depth is obtained from a stationary Markov chain; for example, the noise at the i th level is taken as a fraction of the noise at the $(i-1)$ th channel added to a new random realization passed through the tuned filter. In the model the sharp spectral peak at .25 cps is for highly correlated noise between channels contrasted with that at 2 cps when the noise is uncorrelated between channels. The strong correlation at low frequencies results in a peak which is spread broadly over all wave numbers.

Ambient Noise

The ambient noise spectrum derived from a four minute sample is shown on Figure 16. Comparing this with noise generated from a Markovian process, the .25 and 2.0 cps peaks

```

SPRINKLER NO. 0      1      NO. OF CHANNEL 0  5
SAMPLING RATE 0  20.00  STARTING POINT 0  300  TOTAL POINTS 0  120
THE NUMBER OF SMOOTHING TIME 0

```

CHANNEL ID	SCALE FACTOR	DEPTH	U R	SYMBOL
A1	1.00	.015	0 - 3	0
A2	1.00	1.000	4 - 9	4
A3	1.00	1.000	10 - 10	2
A4	1.00	2.000	10 - 21	0
A5	1.00	2.010	24 - 27	0

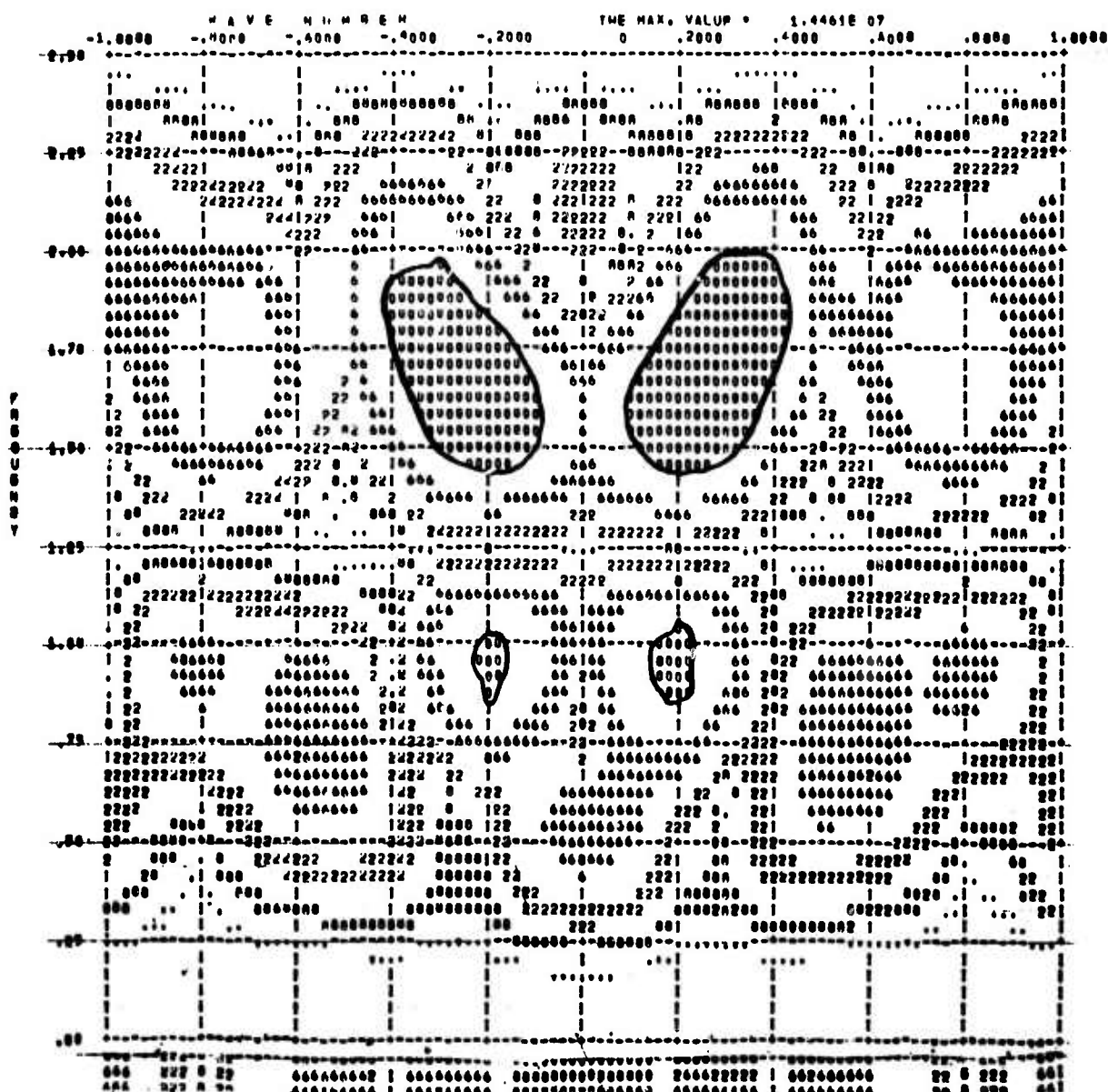


**Figure 14. Simulated Signal Using Acoustic Log
Propagation Velocities Measured at APOK**


```

GEIGHEMAN NO. = 1 NO. OF CHANNEL = 8
SAMPLING RATE = 20.00 STARTING POINT = 1 TOTAL POINTS = 4000
THE NUMBER OF SMOOTHING TIME = 5

```

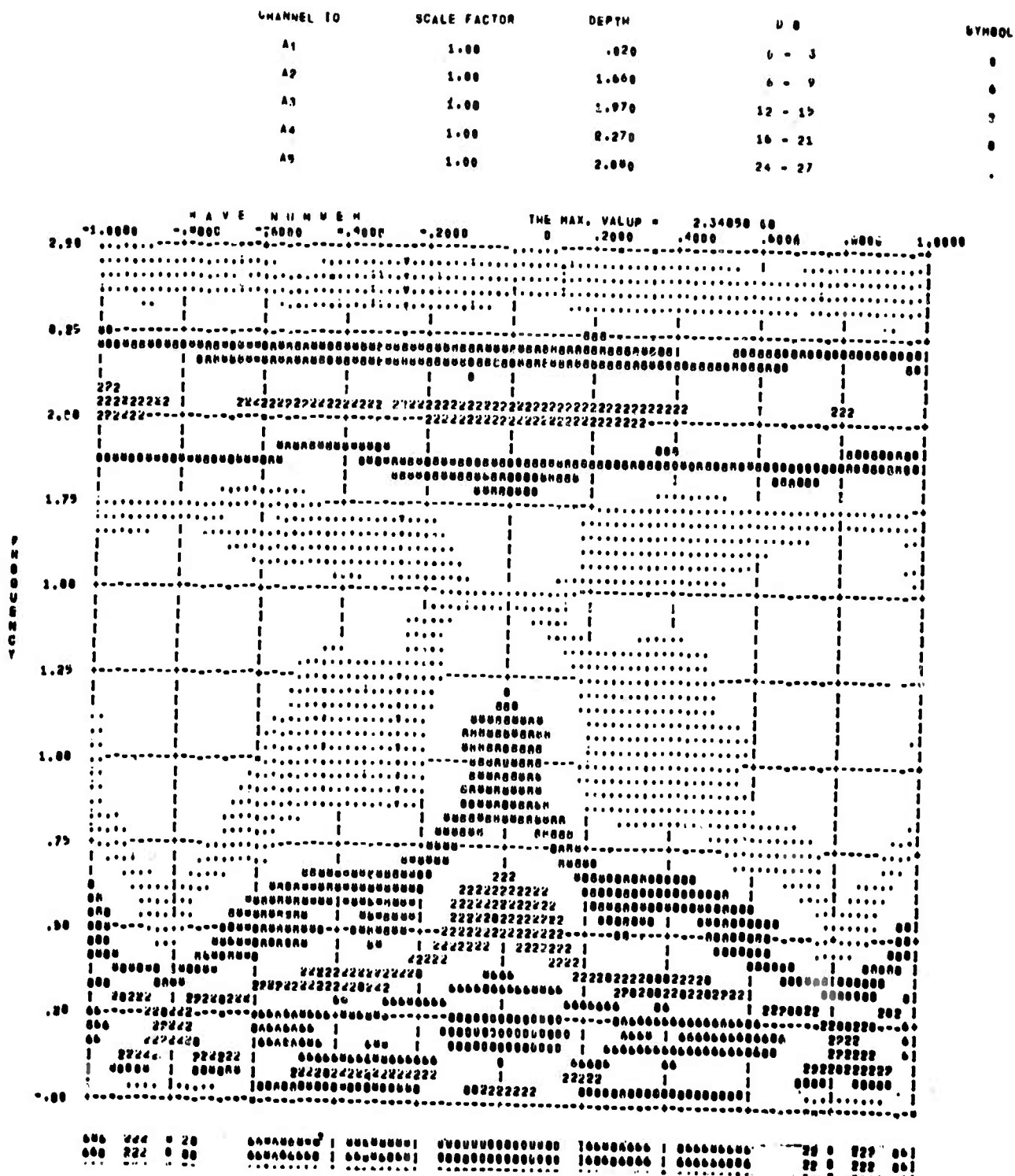
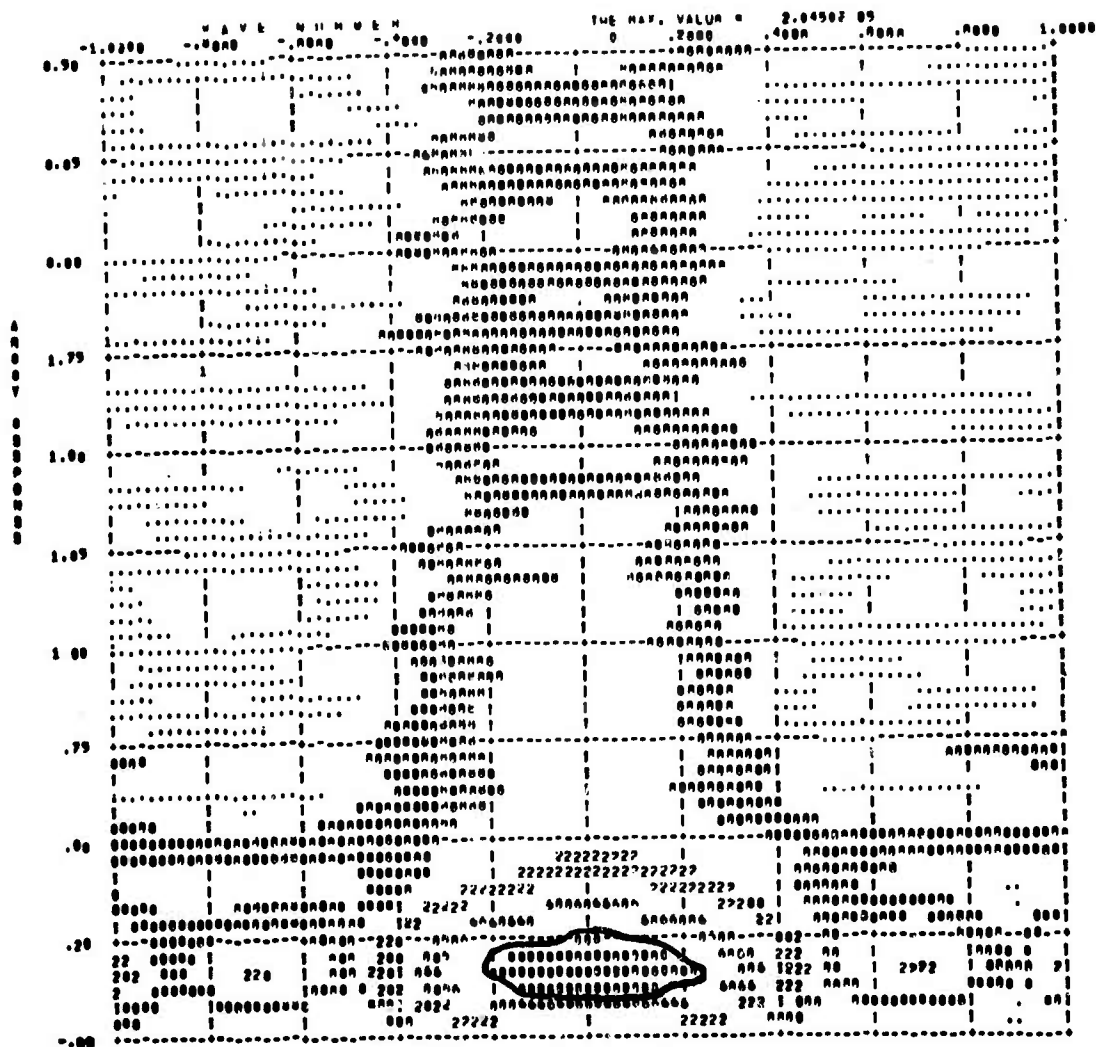


Figure 15. Simulated Noise

VFKSPTRM AMBIENT NOISE, UBO, STARTING AT 6/20/0.0 Z

OBSERVATION NO. = 11681
 NO. OF CHANNEL = 5
 SAMPLING RATE = 80.00 STARTING POINT = 1 TOTAL POINTS = 4004
 TWO MINUTE UP SMOOTHING TIME = 5

CHANNEL NO	SCALE FACTOR	DEPTH	U M	SYMBOL
001	1.00	2.710	9 - J	0
003	1.00	2.110	9 - 0	0
004	1.00	1.000	12 - 14	0
005	1.00	1.400	10 - 21	0
006	1.00	1.130	24 - 27	.



0 000 00 0 00000000 0 1000 000000000000000000 000 2 12222222 1
 0 000 01 0 00000000 2 1000 000000000000000000 000 2 10000000 1 00 000
 0 000 10 0 00000000 2 1000 000000000000000000 000 2 12222222 1 00 000
 0 000 00 0 00000000 0 1000 000000000000000000 000 2 10000000 1 00 000

Figure 16. Unfiltered Noise

are of similar character suggesting very high correlation between channels for the .25 cps peak and very low correlation for the 2.0 cps noise peak. The principal difference between the observed noise at APOK on Figure 16 and the synthetic noise generated using the extremely simple linear state model is a rotation of the whole pattern toward negative wave numbers. This same effect can be produced by inputting the random function to a process which produces negative delays or lead time equal to X/C representing conversion to up-going waves where the apparent vertical phase velocity C is obtained from the slope of the line shown on Figure 16. The value obtained for C is approximately 12 km/sec corresponding to an incidence angle of about 75° . This suggests the possibility of Stonely waves guided upwards along the thick low-velocity layer, dipping 15° . This possibility is qualitatively consistent with the anomalous signal shown on Figure 18.

Other differences between observed noise on Figure 16 and the model on Figure 15 are the three noise peaks at 1.0 cps, 1.4 cps, and 1.6 cps. The 1.0 and 1.4 peaks appear to be highly correlated between channels; the 1.6 shows low correlation in the noise between adjacent channels. These peaks in the signal band appear to have nearly infinite vertical phase velocity and are probably due to Rayleigh waves, i.e., vertical and possibly also horizontal standing waves trapped in the basin bounded by higher velocity basement complex rocks.

A 6-second sample of the earthquake pulse is shown on Figure 18. The up-going pulse gives spectral peaks at .85 cps, 1.20 cps, and 1.9 cps. The apparent vertical phase velocity is approximately the same as that shown by Figure 17 for the noise preceding the signal. Lower than expected vertical phase velocities suggest departure from the model of a pulse and echo based on acoustic log velocities (Figure 14). The apparent velocities are lower by at least fifteen to twenty percent. Also, the down-going earthquake pulse is even more anomalous. The amplitude is down 6 db from that of the up-going pulse; the apparent vertical velocity is very low; and the .85 cps peak down-going phase appears to contain lower frequency. A possible explanation of the anomalous signal can be based on dipping beds.

This may help to explain the anomalous low amplitude down-going reflection. The anomalous apparent vertical velocities may result from forward scattered P-S conversions, especially at the surface, due to anomalously high angle of emergence. Looking again at Figure 18, there appears to be signal peaks at nearly infinite vertical phase velocity.

Figures 16 and 17 show the f-k spectra of two samples of noise recorded at the UBO vertical array. In contrast to that at APOK the character of the noise as seen at UBO shows a high degree asymmetry. Thus the energy conversion or the strongly dipping beds which cause more upgoing than downgoing energy at APOK are not observed to play an important role at the UBO vertical array. There is no obvious indication of reflected P wave noise at UBO although this type of noise may be obscured by the array response.

VFKSPTRM AMBIENT NOISE, UBO, STARTING AT 9/00/00.0 Z
 OBSERVATION NO. = 11092 NO. OF CHANNEL = 5
 SAMPLING RATE = 20.00 STARTING POINT = 1 TOTAL POINTS = 4096
 THE NUMBER OF SOUNDING TIME = 5

CHANNEL ID	SCALE FACTOR	DEPTH	U P	SYMBOL
UW1	1.00	2.710		
UW3	1.00	2.110	0 - 3	0
UW4	1.00	1.800	4 - 9	0
UW5	1.00	1.490	12 - 15	2
UW6	1.00	1.130	18 - 21	0
			24 - 27	.

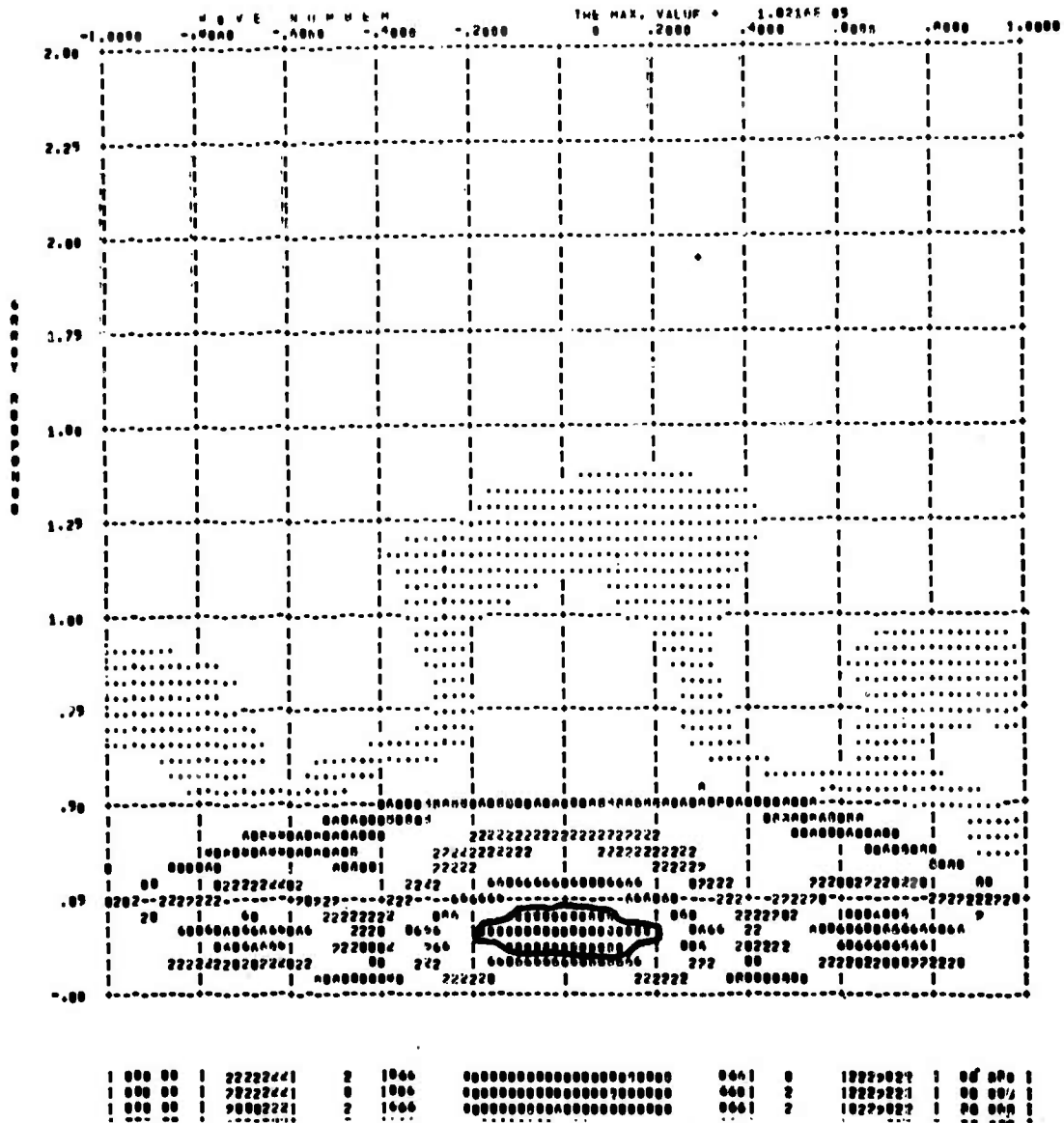


Figure 17. Unfiltered Noise

VTKSPTRM EARTHQUAKE ALEUTIAN ISLAND, STATION APOK

SEISMOGRAM NO. = 6353

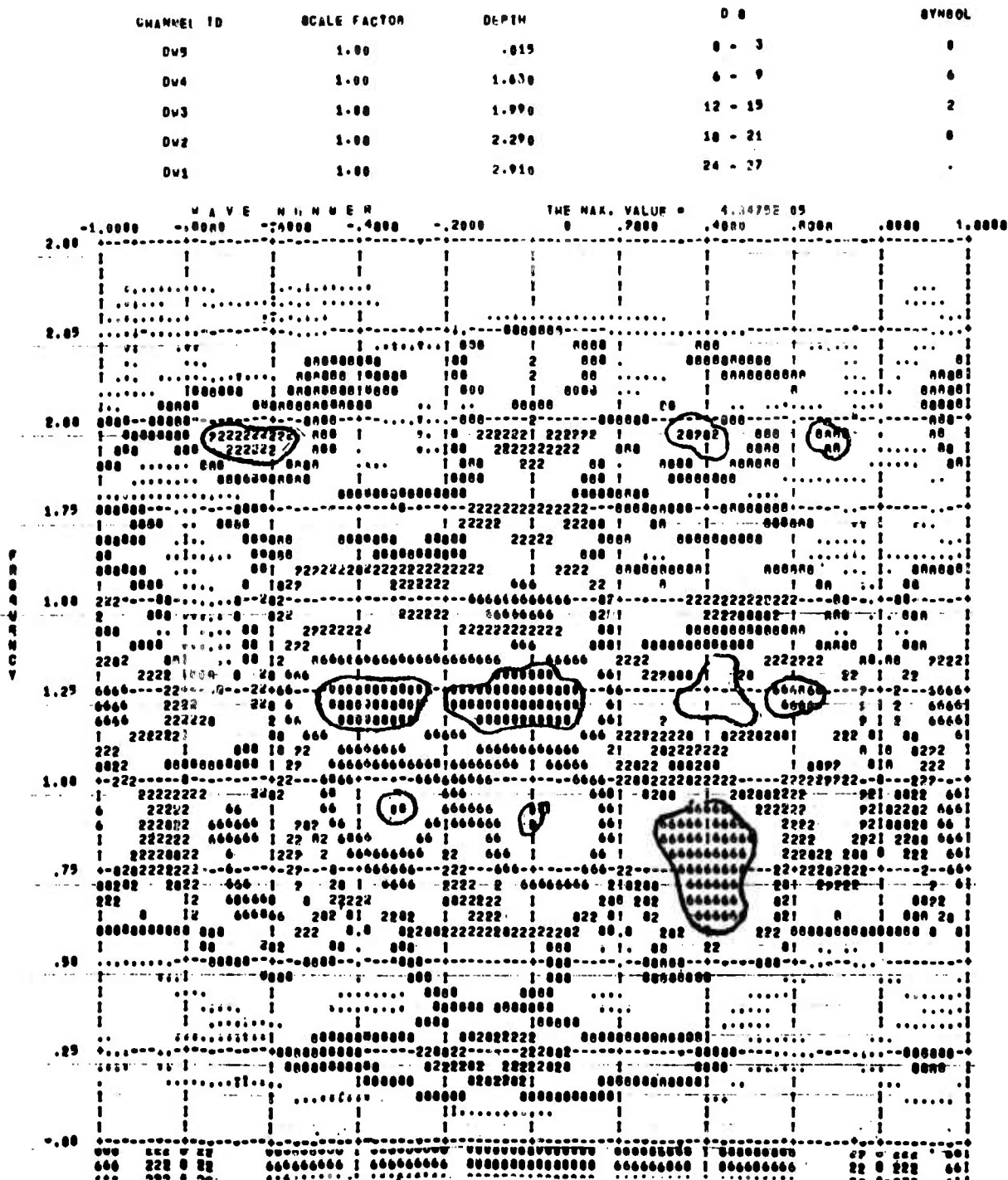
NO. OF CHANNEL = 5

SAMPLING RATE = 80.00

STARTING POINT = 440

TOTAL POINTS = 128

THE NUMBER OF SWEEPING TIME = 0



III. SUPPORT AND SERVICE TASKS

A. VELA-UNIFORM Data Services

As part of the contract work-statement, the SDL provided one or more of the following support and service functions for VSC and other VELA participants:

- copies of 16 and 35 mm film.
- playouts of earthquakes and special events
- copies of existing composite analog tapes
- composite analog tapes of special events
- use of 1604 computer for checking out new programs or running production programs
- copies of digital programs
- digitized data in standard formats or special formats for use on computers other than the 1604
- running SDL production programs, such as power spectral density and array processing one specified data
- digital x-y plots of power spectra or digitized data
- signal reproduction booklets
- space for visiting scientists utilizing SDL facilities to study data and exchange information with SDL personnel.

During this report period, 55 such projects were completed and the 15 organizations receiving these services are listed in Appendix A.

B. Data Library

The Data Library contains approximately 7,000 digitized seismograms. 185 digital computer programs and 293 composite analog magnetic tapes, all available for use by the VELA-UNIFORM program.

The following additions were made during this period.

1. Digital Seismograms - 163 including
 - data from 12 explosions and 3 underwater events
 - noise samples from LASA, TFO, UBSO, CPSO, and WMSO
 - deep well data
 - 37 earthquakes recorded at various stations
2. LASA Data - 86 digital tapes
 - there are a total of 1076 digital tapes in the library including 831 field tapes. There is also a master calibration tape which contains the magnification (digital counts per millimicron) of each sensor for every sub-array. These magnifications have been computed for all calibration tapes currently in house.

As each new calibration is received, it is routinely run through the new program CALIBR and added to the master tape.

3. Digital Programs - 15 including:

BACKFILE - to backspace files on tape.

DPWELLSN - deepwell data processing program for S/N ratio computations.

MERGSEIS - program to merge two seismograms.

PARTLCOH - this program computes partial coherence functions for taped data as well as the amplitude and phase of the assoc. transfer function.

RODBUDSC - the subset program retrieves seismic records, no matter how they are requested, in the same order that they are written on a library tape.

LASACORL - to process LASA seismic data.

POLFIT - the polynomial $Y = B_1 + B_2 X + \dots B_{K+1} X^k$ is fitted for all degrees k , $1 \leq k \leq k_{\max}$ according to the observed independent and dependent variables. A printer plot of Y is obtained with the use of subrouting PLOT.

ISOFIL - this program computes and/or applies a multi-channel isotropic processor to seismic array data. An annular ring noise model and, either a point or a disc signal model, can be specified. The program then solves the multichannel Wiener-Hopf equation in the frequency domain to get the optimum filter which rejects the noise and passes the signal.

SUBSETSL - to subset a packed or unpacked standard SDL library tape, a LASA format tape, or a subset tape.

DESPIKE - to remove spikes from a seismogram by simply inserting a cosine function in a specified interval.

UNPKLTTP - to unpack an SDL standard library tape. Each data point for N channels ($N \leq 4$) is packed as N 12-bit integer values in a parallel manner. By simply shifting an appropriate no. of bits to the far left in the word and then shifting 36 bits to the right justify, the desired 12-bit data point is retrieved.

MEFALUMP - this program computes and/or applies a multichannel isotropic processor to seismic array data. An actual noise model is used computed from the spectra of a specified data sample. Either a point or a disc signal model can be computed. The program then solves the Wiener-Hopf equation in the frequency domain to get the optimum filter which rejects the noise and passes the signal.

MULTICOH - this program computes multiple coherence functions for seismic array data rapidly and efficiently. Given an original set of N subset data channels, the program will compute the N-1 multiple coherence functions:

$$\alpha_i(N-1/N, \dots, N-i+1) \quad i = 1 \dots N-1$$

The program will then reorder the N data channels any number of times, each time computing another N-1 multiple coherence function. The print-out includes a description of the notation used. Optional print-out includes all the auto and cross spectra. In addition a provision exists to plot the multiple coherence functions. The Cooley-Tukey method of spectral estimation is used to obtain high speed.

BULALIST - to add recording stations to a list of earthquakes on magnetic tape.

ATODALL & ATOD20 - conversion of two A to D conversion routines to FORTRAN-63.

4. Analog Composite Tapes - 3 including:

- a. Made by SDL
 - Special UBO composite
- b. Made by Geotech
 - COMMODORE
 - SCOTCH

C. Data Compression

This is a continuing routine operation, and production is maintained at the level needed to meet the requirements of the field operation (LRSM and U. S. Observatories) and the Seismic Data Laboratory. For this period, 2,515 tapes were compressed.

D. Automated Bulletin Process

April, May, and June 1967 LRSM and Observatory bulletins were processed during this report period and forwarded to Geotech, A Teledyne Company, for checking and publication.

REFERENCES

1. Broome, P.W., Frankowski, D.E., and Klappenberger, F.A., 9 January, 1967, "Amplitude Anomalies at LASA", Report No. LL-4, Applied Research, Teledyne, Inc., Alexandria, Virginia.
2. Klappenberger, F.A., 9 June, 1967, "Distribution of Short Period P-Phase Amplitudes over LASA", Report No. 187, Teledyne, Inc., Alexandria, Virginia.

APPENDIX A

ORGANIZATIONS RECEIVING SDL DATA SERVICES

July - September 1967

California Institute of Technology

Colorado School of Mines

Earth Sciences, Teledyne

General Atronics Corporation

Geotech, Teledyne

Hollaman Air Force Base

IBM Corporation

Lamont Geophysical Observatory

Lawrence Radiation Laboratory

Lincoln Laboratory, MIT

Oregon State University

Penn State University

Texas Instruments, Inc.

U. S. Coast and Geodetic Survey

Vitro Corporation

Unclassified

Security Classification

DOCUMENT CONTROL DATA - R&D		
(Security classification of title, body of abstract and indexing annotation must be entered when the overall report is classified)		
1. ORIGINATING ACTIVITY (Corporate author) TELEDYNE, INC. ALEXANDRIA, VIRGINIA		2a. REPORT SECURITY CLASSIFICATION Unclassified 2b. GROUP ----
3. REPORT TITLE SEISMIC DATA LABORATORY QUARTERLY TECHNICAL SUMMARY REPORT		
4. DESCRIPTIVE NOTES (Type of report and inclusive dates) Quarterly Summary - July - September 1967		
5. AUTHOR(S) (Last name, first name, initial) Dean, William C.		
6. REPORT DATE 24 October 1967	7a. TOTAL NO. OF PAGES 42	7b. NO. OF REFS 2
8a. CONTRACT OR GRANT NO. F33657-67-C-1313 8. PROJECT NO. VELA T/6702 9. ARPA Order 624 4ARPA Program Code No. 5810	9a. ORIGINATOR'S REPORT NUMBER(S) --- 9b. OTHER REPORT NO(S) (Any other numbers that may be assigned this report) Technical Summary Report No. 17	
10. AVAILABILITY/LIMITATION NOTICES This document is subject to special export controls and each transmittal to foreign governments or foreign national may be made only with prior approval of Chief, AFTAC.		
11. SUPPLEMENTARY NOTES ----	12. SPONSORING MILITARY ACTIVITY ADVANCED RESEARCH PROJECTS AGENCY NUCLEAR TEST DETECTION OFFICE WASHINGTON, D. C.	
13. ABSTRACT This report discusses the work performed by SDL for the period July through September 1967, and is primarily concerned with seismic research activities leading to the detection and identification of nuclear explosions as distinguished from earthquake phenomenon. Also discussed are the data services performed for other participants in the VELA-UNIFORM project.		

DD FORM 1473
1 JAN 64

Unclassified

Security Classification

Unclassified

Security Classification

14

KEY WORDS

Seismic Data Laboratory - Quarterly
 Technical Summary
 VELA-UNIFORM Project
 Seismic Noise
 Amplitude Anomalies
 Beamforming
 E3 Subarray

LINK A

LINK B

LINK C

ROLE

WT

ROLE

WT

ROLE

WT

INSTRUCTIONS

1. **ORIGINATING ACTIVITY:** Enter the name and address of the contractor, subcontractor, grantee, Department of Defense activity or other organization (corporate author) issuing the report.

2a. **REPORT SECURITY CLASSIFICATION:** Enter the overall security classification of the report. Indicate whether "Restricted Data" is included. Marking is to be in accordance with appropriate security regulations.

2b. **GROUP:** Automatic downgrading is specified in DoD Directive 5200.10 and Armed Forces Industrial Manual. Enter the group number. Also, when applicable, show that optional markings have been used for Group 3 and Group 4 as authorized.

3. **REPORT TITLE:** Enter the complete report title in all capital letters. Titles in all cases should be unclassified. If a meaningful title cannot be selected without classification, show title classification in all capitals in parenthesis immediately following the title.

4. **DESCRIPTIVE NOTES:** If appropriate, enter the type of report, e.g., interim, progress, summary, annual, or final. Give the inclusive dates when a specific reporting period is covered.

5. **AUTHOR(S):** Enter the name(s) of author(s) as shown on or in the report. Enter last name, first name, middle initial. If military, show rank and branch of service. The name of the principal author is an absolute minimum requirement.

6. **REPORT DATE:** Enter the date of the report as day, month, year; or month, year. If more than one date appears on the report, use date of publication.

7a. **TOTAL NUMBER OF PAGES:** The total page count should follow normal pagination procedures, i.e., enter the number of pages containing information.

7b. **NUMBER OF REFERENCES:** Enter the total number of references cited in the report.

8a. **CONTRACT OR GRANT NUMBER:** If appropriate, enter the applicable number of the contract or grant under which the report was written.

8b, 8c, & 8d. **PROJECT NUMBER:** Enter the appropriate military department identification, such as project number, subproject number, system numbers, task number, etc.

9a. **ORIGINATOR'S REPORT NUMBER(S):** Enter the official report number by which the document will be identified and controlled by the originating activity. This number must be unique to this report.

9b. **OTHER REPORT NUMBER(S):** If the report has been assigned any other report numbers (either by the originator or by the sponsor), also enter this number(s).

10. **AVAILABILITY/LIMITATION NOTICES:** Enter any limitations on further dissemination of the report, other than those

imposed by security classification, using standard statements such as:

- (1) "Qualified requesters may obtain copies of this report from DDC."
- (2) "Foreign announcement and dissemination of this report by DDC is not authorized."
- (3) "U. S. Government agencies may obtain copies of this report directly from DDC. Other qualified DDC users shall request through _____."
- (4) "U. S. military agencies may obtain copies of this report directly from DDC. Other qualified users shall request through _____."
- (5) "All distribution of this report is controlled. Qualified DDC users shall request through _____."

If the report has been furnished to the Office of Technical Services, Department of Commerce, for sale to the public, indicate this fact and enter the price, if known.

11. **SUPPLEMENTARY NOTES:** Use for additional explanatory notes.

12. **SPONSORING MILITARY ACTIVITY:** Enter the name of the departmental project office or laboratory sponsoring (paying for) the research and development. Include address.

13. **ABSTRACT:** Enter an abstract giving a brief and factual summary of the document indicative of the report, even though it may also appear elsewhere in the body of the technical report. If additional space is required, a continuation sheet shall be attached.

It is highly desirable that the abstract of classified reports be unclassified. Each paragraph of the abstract shall end with an indication of the military security classification of the information in the paragraph, represented as (TS), (S), (C), or (U).

There is no limitation on the length of the abstract. However, the suggested length is from 150 to 225 words.

14. **KEY WORDS:** Key words are technically meaningful terms or short phrases that characterize a report and may be used as index entries for cataloging the report. Key words must be selected so that no security classification is required. Identifiers, such as equipment model designation, trade name, military project code name, geographic location, may be used as key words but will be followed by an indication of technical context. The assignment of links, rules, and weights is optional.

Unclassified

Security Classification